



OPEN ACCESS

EDITED BY
Santosha Rathod,
Indian Institute of Rice Research (ICAR), India

Santosh Ganapati Patil, Tamil Nadu Agricultural University, India Rahul Patil, University of Agricultural Sciences Raichur,

*CORRESPONDENCE Vinavaka

[†]These authors have contributed equally to this work

RECEIVED 07 August 2025 ACCEPTED 21 October 2025 PUBLISHED 05 November 2025

CITATION

India

Vinayaka, Prasad PRC, Avinash G, Amaresh, Arun Kumar R, Murali P, Palaniswami C and Govindaraj P (2025) Harnessing Al and Remote sensing for precision sugarcane farming: tackling water stress, salinity, and nitrogen challenges. *Front. Agron.* 7:1681294. doi: 10.3389/fagro.2025.1681294

COPYRIGHT

© 2025 Vinayaka, Prasad, Avinash, Amaresh, Arun Kumar, Murali, Palaniswami and Govindaraj. This is an open-access article distributed under the terms of the Creative Commons Attribution License (CC BY). The use, distribution or reproduction in other forums is permitted, provided the original author(s) and the copyright owner(s) are credited and that the original publication in this journal is cited, in accordance with accepted academic practice. No use, distribution or reproduction is permitted which does not comply with these terms.

Harnessing AI and Remote sensing for precision sugarcane farming: tackling water stress, salinity, and nitrogen challenges

Vinayaka^{1*}, P. Rama Chandra Prasad^{2†}, G. Avinash^{3†}, Amaresh^{4†}, R. Arun Kumar⁵, P. Murali¹, C. Palaniswami⁶ and P. Govindaraj⁴

¹Statistics and Economics Section, ICAR-Sugarcane Breeding Institute, Tamil Nadu, India, ²Lab for Spatial Informatics, International Institute of Information Technology, Gachibowli, Telangana, India, ³Executive Chairman & CEO, Avyagraha Research and Analytics LLP, Ramasagara, Karnataka, India, ⁴Division of Crop Improvement, ICAR-Sugarcane Breeding Institute, Tamil Nadu, India, ⁶Soil Science Section, ICAR-Sugarcane Breeding Institute, Tamil Nadu, India, ⁶Soil Science Section, ICAR-Sugarcane Breeding Institute, Tamil Nadu, India

Sugarcane is a vital cash crop with substantial significance in both global sugar production and the biofuel industry. However, its sustainable cultivation faces persistent challenges from environmental stressors, particularly salinity and water scarcity. In recent years, the integration of artificial intelligence (AI) and remote sensing (RS) technologies has proven to be a transformative approach for detecting and evaluating these stress conditions, offering critical insights for advancing precision agriculture (PA). This review explores the utilization of satellite imagery and sensor-based data including RGB, multispectral, hyperspectral imaging, and unmanned aerial vehicles (UAVs) to monitor stressrelated parameters in sugarcane farming. It emphasizes key indices used to assess water stress, generate salinity stress maps, and estimate nitrogen levels, demonstrating their role in equipping farmers with actionable information to optimize irrigation and nutrient management strategies. These innovations significantly enhance crop productivity while promoting environmental sustainability. The review sets out three core objectives: (i) to evaluate the contribution of AI and RS in assessing water stress in sugarcane cultivation, (ii) to examine methods for mapping salinity stress using RS and AI tools, and (iii) to highlight the relevance of spectral indices in tracking nitrogen status in sugarcane crops. Drawing upon reputable bibliographic sources such as Google Scholar, Scopus, ResearchGate, and Web of Science, along with current literature on Al and RS applications in sugarcane stress assessment, the review consolidates detailed information on advanced sensors and UAV technologies. It also introduces novel deep learning models and sensor platforms that have received limited attention in prior studies. In conclusion, the review affirms that Al-driven remote sensing is a highly effective approach for monitoring and

managing critical stress factors in sugarcane production. It not only contributes to enhanced yield and crop quality but also delivers significant socio-economic and environmental benefits, marking a major step forward in achieving sustainable and efficient sugarcane cultivation.

KEYWORDS

Al-driven remote sensing, climate change, crop water stress index, leaf nitrogen content, salinity stress, sugarcane agriculture

1 Introduction

Sugarcane (Saccharum officinarum L.) belongs to the Andropogoneae species within the Poaceae family (Grof and Campbell, 2001). It is a crop of considerable economic importance, primarily cultivated in tropical and subtropical regions (Driemeier et al., 2016). According to recent estimates from the Food and Agriculture Organization (FAO) and the USDA, global raw sugar production for the 2023 - 24 marketing year is expected to surpass 183.5 million tonnes, marking a steady rise from 179 million tonnes in 2019 (FAO, 2022). Further projections estimate a production of approximately 186 million tonnes in 2024 - 25, spurred by increased output in countries like Thailand, India, and China (Infomerics Valuation and Rating Pvt. Ltd, 2024). Beyond its primary use in sugar production, sugarcane serves as a most important biological resource for creating ethanol, bagasse, fiber, molasses, rum, and cachaca (Vinayaka and Prasad, 2024; Amaresh et al., 2024; Suresha et al., 2024). Enhancing agricultural productivity remains a core focus of precision agriculture (PA), influenced by multiple environmental and agronomic factors (Amarasingam et al., 2022; Soltanikazemi et al., 2022). However, sugarcane cultivation is frequently challenged by abiotic stresses such as salinity and water scarcity, which negatively impact both yield and crop quality. The crop accounts for around 29% of global agricultural water use (Milagro Jorrat et al., 2018), and nearly 60% of sugarcane-growing areas in India experience water limitations often due to insufficient irrigation, canal closures during summer, and recurrent droughts (Sundara et al., 2002). Developing water-efficient sugarcane genotypes is essential for sustaining production while improving regional and global water security (Tayade et al., 2020; Kumar et al., 2020). Salinity poses a parallel threat: globally, approximately 33% of irrigated land and 20% of cultivated land are affected by saline conditions. In India, sugarcane is cultivated on nearly 5 million hectares, with about 25% of this area impacted by salinity, alkalinity, or saline irrigation water (Vasantha and Gomathi, 2012).

Remote sensing (RS) has become an indispensable tool in crop stress monitoring due to its ability to capture high-resolution, large-scale data (Huang et al., 2018). The accurate assessment of water, salinity, and nitrogen stress in sugarcane is decisive for informed crop management. Water deficits can significantly reduce

productivity, underscoring the importance of precise irrigation scheduling (Hamzeh et al., 2013). Likewise, salinity stress caused by high salt concentrations in soil can hinder plant growth and yield potential (Hamzeh et al., 2016). Early detection allows for timely mitigation strategies such as leaching or improved drainage (Patil et al., 2021; Watanabe et al., 2022). Leaf nitrogen content (LNC) serves as a pivotal indicator of crop health and nutritional balance. Nitrogen deficiency limits growth and productivity, whereas excess application can cause environmental damage (Anas et al., 2020). Accurate monitoring of LNC supports optimized fertilization strategies, promoting sustainable practices (Virnodkar et al., 2020). Hence, evaluating water, salinity, and nitrogen stress is essential for improving sugarcane performance (Ferreira et al., 2017; Kumar et al., 2023b). Water stress in sugarcane is often attributed to erratic rainfall, exposure to alternating wet and dry periods, and high evapotranspiration rates (Bispo et al., 2022; Brunini and Turco, 2016). The concept of Crop Water Stress (CWS), introduced by Idso et al. (1981), has become a standard for assessing water deficits at both leaf and canopy levels. Salinity stress can arise from saline soil layers, the use of brackish irrigation water, elevated groundwater tables, or seawater intrusion (Hamzeh et al., 2016), contributing to widespread soil degradation in sugarcane-growing regions (Hamzeh et al., 2013). High water tables exacerbate this problem by raising salinity to damaging levels, thereby reducing crop output (Hamzeh et al., 2012). To mitigate such stresses, precision irrigation techniques and real-time monitoring of soil moisture and crop development are crucial (Yang H. et al., 2019). Additionally, salt removal from the root zone and field-specific corrective measures are necessary to maintain productivity (Burt and Isbell, 2005). Artificial intelligence (AI) and RS play complementary roles in assessing water and salinity stress in sugarcane. RS techniques such as thermal imaging and satellite-based data are valuable for estimating evapotranspiration (ET) and managing irrigation systems (Hamzeh et al., 2016; Das et al., 2020; Bispo et al., 2022; Watanabe et al., 2022). Energy balance models and vegetation indices are used to estimate ET and detect crop water stress (Patil et al., 2021; Virnodkar et al., 2021). Meanwhile, AI approaches, particularly machine learning (ML) and convolutional neural networks (CNNs), have shown promise in analyzing RS data to classify and map stress-affected zones in sugarcane fields. Nitrogen (N) remains a critical determinant of sugarcane yield and quality (Wiedenfeld,

1995), influencing attributes such as photosynthesis, tiller production, stem length, and girth (Gopalasundaram et al., 2012). Effective nitrogen management is thus central to sustainable productivity (Boschiero et al., 2020; Yang Y. et al., 2019). Extensive research on the optimal application of nitrogen fertilizers in sugarcane cultivation has been conducted globally, considering factors like growth cycle, climatic conditions, cultivar, and soil properties (Meyer et al., 1986; Wood et al., 1996). Although traditional techniques such as chlorophyll meters, soil sampling, and tissue analysis exist, they are often unsuitable for large-scale use due to their invasive, costly, and time-consuming nature (Ranjan et al., 2012).

Recent advances in AI and RS have facilitated non-invasive estimation of foliar nitrogen. Hyperspectral imagery, sensitive to biochemical changes in vegetation, has been effectively employed for nitrogen assessment (Soltanikazemi et al., 2022). Indices such as the Global Environmental Monitoring Index (GEMI), Chlorophyll Green Index (Clgreen), and Sentinel-2 Red-Edge Position Index (S2REP) have proven useful in estimating nitrogen levels in sugarcane leaves (Abdel-Rahman et al., 2013). Feature selection algorithms like Random Forest (RF) help reduce redundancy in hyperspectral datasets (Abdel-Rahman et al., 2010), while AI models including RF and Support Vector Regression (SVR) have demonstrated success in predicting nitrogen content rapidly and accurately (Martins et al., 2024). These methods offer practical, cost-effective, and scalable solutions for nitrogen monitoring (Bispo et al., 2022). Conventional stress monitoring techniques often lack the precision and speed required for proactive decision-making, reinforcing the need for advanced technologies. This review, therefore, emphasizes AI-based RS solutions for assessing key stressors in sugarcane agriculture. The primary objectives of this article are to: (i) explore how RS and AI are applied in sugarcane farming to evaluate crop water stress, (ii) investigate methods for mapping salinity stress using integrated RS and AI approaches, and (iii) highlight how spectral indices and AI tools can be leveraged to monitor the nitrogen status of sugarcane crops. Accordingly, the article is structured as follows: Section 2 covers bibliographic analysis; Section 3 presents a detailed discussion on integrated AI-RS methodologies and statistical software, along with recommendations for evaluating nitrogen, salinity, and water stress; Section 4 addresses existing challenges and limitations; Section 5 outlines future research directions; and Section 6 offers concluding insights.

2 Literary examination of sources

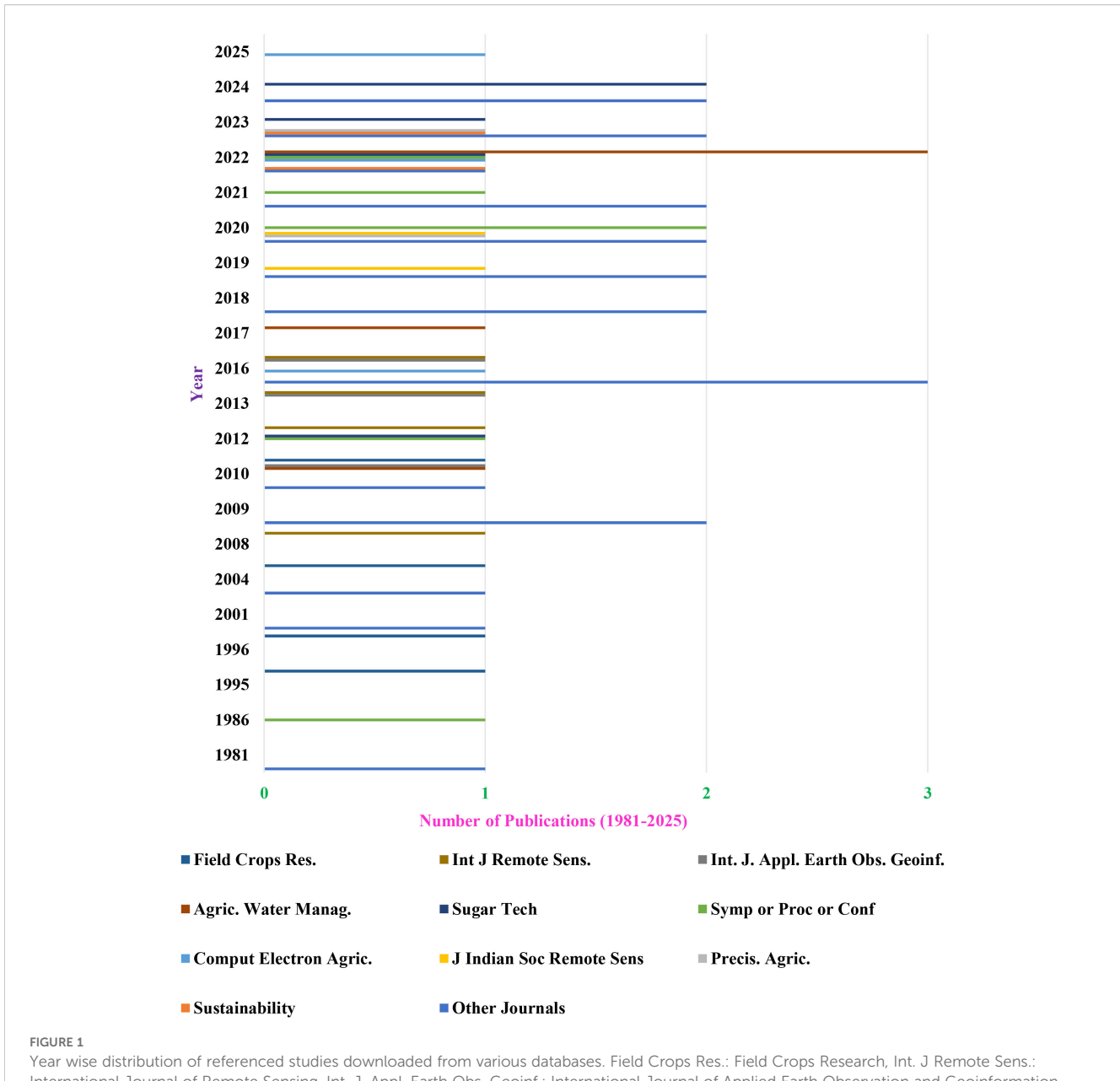
This study offers a comprehensive review of research focused on key stressors namely water stress, salinity stress, and plant nitrogen deficiency within the context of sugarcane cultivation. The review encompasses various aspects such as leaf nitrogen estimation, detection of water and salinity stress, and associated spectral signatures and vegetation indices. It particularly emphasizes the role of AI and RS technologies in addressing these challenges, highlighting recent advancements, practical applications, and the

benefits and limitations of these approaches in sugarcane agriculture. To ensure a thorough evaluation, an extensive literature search was conducted using multiple academic databases, including Google Scholar, Scopus, ResearchGate, and Web of Science. The search focused on publications from 1981 to 2025, drawing upon peer-reviewed research articles, book chapters, and review papers. A total of 72 relevant sources (out of 88 references) were identified and systematically organized. Of these, 36 publications specifically demonstrated the effective application of AI, RS, or integrated approaches in various sugarcane-related domains such as water stress detection, leaf nitrogen monitoring, and salinity stress evaluation (Figure 1, Figure 2).

Journal titles have been abbreviated following the ISO4 standard, with a few exceptions such as Plan Plus, Water SA, Sustainability, Sugar Tech, and FAO Annual Report. The review also incorporates valuable content from symposium articles (Symp), conference proceedings (Proc), and conference papers (Conf). A strategic search methodology was adopted to compile the bibliography. Specific keywords and key phrases were used either individually or in logical combinations to locate relevant material. These included: "crop water stress", "water stress of sugarcane assessment using AI/ML/DL and remote sensing", "salinity stress", "salinity stress of sugarcane assessment using AI/ ML/DL and remote sensing", "leaf nitrogen estimation in sugarcane using AI/ML/DL and remote sensing", "drought detection", "plant nitrogen stress", "evapotranspiration", "water productivity", "water balance", "water deficit". These search terms enabled the retrieval of a broad and diverse set of studies on AI and RS applications in sugarcane management. Figure 3 illustrates a word frequency analysis of the selected references, focusing on the prominence of AI-based RS research in sugarcane stress management. Notably, several recent publications also served as entry points for accessing foundational works and earlier studies, offering deeper insight into the evolution of the field.

3 Detailed critiques

The utilization of RS applications in sugarcane farming encompasses a wide range of aspects, including crop classification, harvest planning, yield forecasting, disease detection and management (Palaniswami et al., 2011; 2014; Vinayaka and Prasad, 2024), assessment of crop health and growth, and detection of CWS. Among these, CWS detection plays a crucial role in predicting yield potential and optimizing irrigation scheduling across different growth stages and seasons. Various methodologies have been developed for identifying CWS, integrating soil water measurements, plant physiological responses, and RS techniques. The present study provides a comprehensive review of global approaches for detecting water stress in sugarcane using diverse RS methods and ML algorithms. The compiled indices (Table 1) illustrate the breadth of RS-based approaches employed for evaluating water status in irrigated sugarcane fields, reflecting the dynamic and adaptable nature of water stress assessment methods.

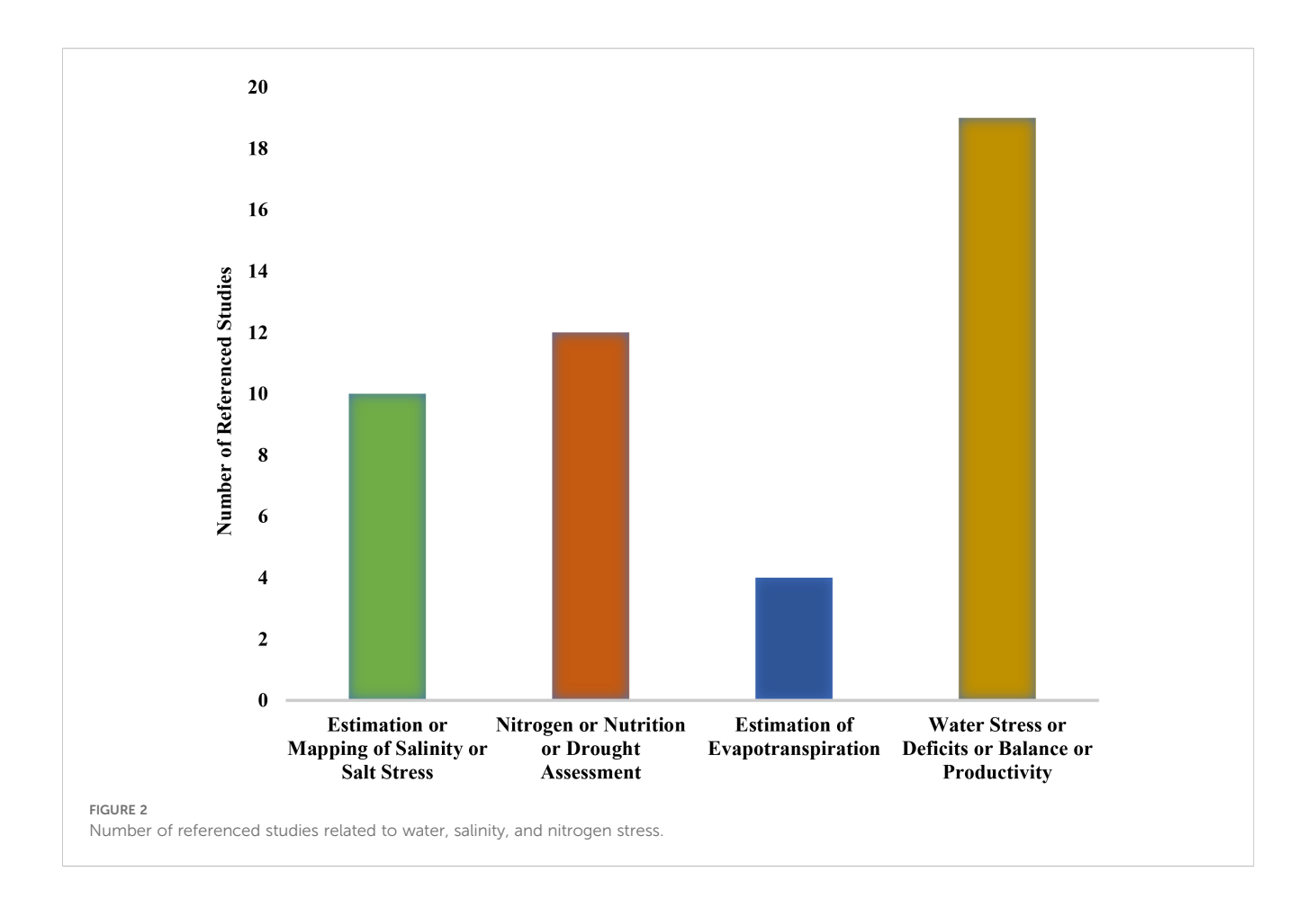


Year wise distribution of referenced studies downloaded from various databases. Field Crops Res.: Field Crops Research, Int. J Remote Sens.: International Journal of Remote Sensing, Int. J. Appl. Earth Obs. Geoinf.: International Journal of Applied Earth Observation and Geoinformation, Agric. Water Manag.: Agricultural Water Management, Symp or Proc or Conf: Symposium/Proceedings/Conference Papers, Comput Electron Agric.: Computers and Electronics in Agriculture, J Indian Soc Remote Sens: Journal of the Indian Society of Remote Sensing, Precis. Agric.: Precision Agriculture.

Advancements in precision agriculture have further expanded the role of RS through the integration of AI and the Internet of Things (IoT), jointly termed AIoT-based water management. These systems leverage real-time data from soil moisture and weather sensors to optimize irrigation schedules, significantly enhancing water-use efficiency (Yueanket et al., 2024). Predictive algorithms such as Long Short-Term Memory (LSTM) models forecast irrigation requirements based on crop growth stages, thereby minimizing water wastage and promoting sustainable resource use. RS complements these systems by providing high-resolution imagery from satellites and drones for spatiotemporal monitoring of crop health and water stress through indices such as Normalized Difference Vegetation Index (NDVI)

(Pawar et al., 2024). Moreover, thermal and hyperspectral imaging enable precise monitoring of environmental stressors, facilitating timely interventions (Swami et al., 2025; Cho et al., 2024).

Beyond water management, RS techniques have also been effectively employed for salinity stress and nitrogen status assessment in sugarcane. High soil salinity adversely affects plant growth, yield, and overall crop health, making its evaluation essential for sustainable production. Table 2 presents an overview of the RS-based indices and approaches commonly used for salinity stress assessment in sugarcane. Similarly, estimation of LNC is pivotal for optimizing fertilizer application and ensuring optimal growth and yield. Spectral reflectance measurements, vegetation



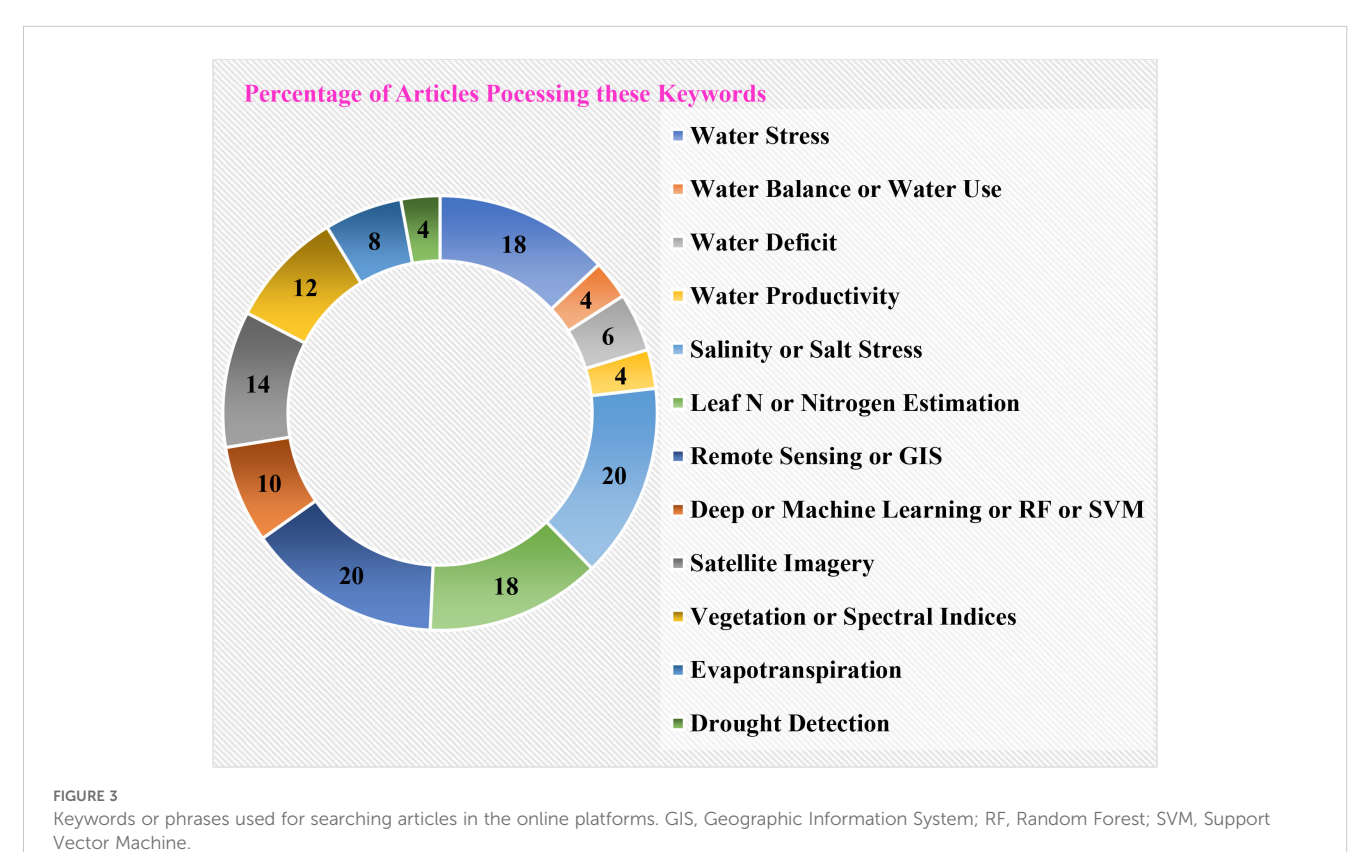


TABLE 1 Vegetation or spectral indices used in the referenced studies for crop water stress estimation.

Author(s)	Expression(s)/indices	Abbreviation & description
Inman-Bamber (2004)	SWD = (drained upper limit) – (soil water content) and Cumulative $ET_0 = \sum ET_0$	SWD (soil water deficit), and ET_0 (daily reference evaporation)
Hellegers et al. (2009)	$\begin{split} CWP_i &= Y_i/ET_{acti} \\ EWP_i &= (P_i \times Y_i \times B_i \times Y_i \times C_i) = ET_{acti} \\ \text{where, } Y_i \text{ Yield of crop } i \text{ (kg/ha)} \\ P_i \text{ Market price received for crop } i \text{ ($/kg)} \\ B_i \text{ Variable production cost of crop } i \text{ ($/kg)} \\ C_i \text{ Fixed production cost of crop } i \text{ ($/ha)} \end{split}$	CWP (crop water productivity), and EWP (economic water productivity)
Singels et al. (2010)	i). $SWDF_i = f_i \times (WSp/Tmax)$ [bound by $0.0 \le SWDF_i \le 1.0$] where fi is a process-specific parameter, usually with a value between 0.0 and 1.0 ; WSp is potential crop water uptake (i.e., potential supply) and $Tmax$ is maximum transpiration (i.e., demand) ii). $SWDFi = (1/p_i) \times RASW$ where, $RASW$ is the relative available soil water content of the root zone; pi is the $RASW$ value where process i is reduced below the potential rate ($p_1 = 0.45$ for carbon assimilation, $p_2 = 0.55$ for structural growth and $p_3 = 0.5$ for water uptake).	SWDF (soil water stress factors)
Lebourgeois et al. (2010)	$CWSI_{e} = ((Tc-Ta)m-(Tc-Ta)ll)/((Tc-Ta)ul-(Tc-Ta)ll) \\ here, lower baseline (ll) denotes "non-water-stressed baseline", which is VPD \\ dependent, and the upper baseline (ul) represents (Tc - Ta) for a canopy with no transpiration and is VPD independent, and (Tc - Ta)m is the measured difference between canopy and air temperature.$	CWSI _e (empirical crop water stress index)
Teixeira et al. (2016)	$ET_r = \left[\exp\left\{a_{sf} + b_{sf}(\frac{T_S}{\alpha_0 NDVI})\right\}\right] \frac{ET_{0-GC}}{5} \text{ where a_{sf} and b_{sf} are regression coefficients,}$ respectively. The correction factor (ET_{0-GC}/5) was applied for atmospheric demand calibration, being ET_{0-GC} the daily ET_0 grid for sugarcane GC and 5 mmd $^{-1}$ is the ET_0 daily average for the same period during the original modeling condition. $NDVI = \frac{\alpha_2 - \alpha_1}{\alpha_2 + \alpha_1}; \text{ and } T_S = \sqrt[4]{R_S/\sigma\varepsilon_S} \text{ where } \alpha_2 \text{ and } \alpha_1 \text{ denotes reflectances over the}$ ranges of wavelengths in the near infrared (NIR) and red (RED) regions of the solar spectrum, respectively. R_s is surface emitted long-wave radiation, ε_S is surface emissivity, and σ =5.67×10 $^{-8}$ Wm $^{-2}$ K $^{-4}$ (Stefan-Boltzmann constant).	$\mathrm{ET_r}$ (evapotranspiration), and NDVI (normalized difference vegetation index)
Brunini and Turco (2016)	DWSI = Tc - Ta where, Tc = temperature of the vegetal cover (°C); and Ta = air temperature (°C).	DWSI (daily water stress index)
Veysi et al. (2017)	$CWSI = (T_S - T_{Cold})/(T_{Hot} - T_{Cold}) \mbox{where, } T_s \mbox{ is canopy temperature in cropped land,} \\ T_{Cold} \mbox{ is temperature of well-irrigated pixel which is almost covered fully by vegetation} \\ (Cold pixel), \mbox{ and } T_{Hot} \mbox{ is temperature of crop covered pixel with maximum amount of water stress (Hot pixel).} \\ VWC = (FW - DW/DW) \times 100 \\ \mbox{where, } FW = \mbox{fresh weight, } DW = \mbox{dry weight.} \\ \label{eq:weight}$	CWSI (crop water stress index), and VWC (vegetation water content)
Singels et al. (2018)	$DSI = \frac{1}{N} \sum$ $(1 - Fvd)$; $WLI = \frac{1}{N} \sum$ $(1 - Fvw)$ where N is number of days with measured probe data within a given week (usually 7), Fvd and Fvw represent the severity of drought and waterlogging stress, respectively $(1 = \text{no stress}, 0 = \text{severely stressed})$ on a given day.	DSI (drought stress index), and WLI (waterlogged stress index)
Picoli et al. (2019)	$\begin{aligned} &\text{NDVI} = \text{NIR-RED/NIR+RED} \\ &\text{GVMI} = \frac{(NIR+0.1) - (SWIR+0.02)}{(NIR+0.1) + (SWIR+0.02)} \text{NDII} \text{ (SWIR 1)} = \text{NIR-SWIR/NIR+SWIR} \\ &\text{NDII (SWIR 2)} = \frac{NIR - SWIR2}{NIR + SWIR2} \text{VCI} = 100 & \times (\frac{NDVIi - NDV \text{ Im } in}{NDVItext \text{ max} - NDVItext \text{ min}}) \text{NEW} = \\ &\text{RED-SWIR/RED+SWIR} \\ &\text{NEW2} = \text{RED-SWIR2/RED+SWIR2} \end{aligned}$	NDII (normalized diference infrared index), GVMI (global vegetation moisture index), VCI (vegetation condition index), and NEW & NEW2 (2 new indices using NIR and SWIR data)
Waqas et al. (2019)	$IWR = \sum_{i=1}^{n} K_{C_i} \times ET_p \times CA \text{ where, CA}_i \text{ is cropping area of corresponding crop i, in ha.}$ Kc is crop coefficient and ET _p is reference evapotranspiration in m/growing season.	IWR (irrigation water requirement)
Pereira et al. (2020)	$TS = TB_{10} + C_1(TB_{10} - TB_{11}) + C_2 (TB_{10} - TB_{11})^2 + C_0 + (C_3 + W C_4) (1 - \varepsilon) + (C_5 + C_6 W)\Delta \varepsilon$ where TB ₁₀ and TB ₁₁ are brightness temperatures of bands 10 and 11 (° C); C_{ij} $i = 0, 2,, 6$ are parameters of the Split Window algorithm; $\varepsilon =$ mean emissivity; and $\Delta \varepsilon =$ emissivity difference in bands.	T _S (Land surface temperature, °C)

(Continued)

TABLE 1 Continued

Author(s)	Expression(s)/indices	Abbreviation & description
Triadi et al. (2020)	$CWSI = (T_S - T_{Cold})/(T_{Hot} - T_{Cold})$	CWSI
Das et al. (2020)	$\begin{split} ET_c \text{ is expressed as:} \\ (1-Y_a/Y_m) &= K_y (1-ET_c/ET_m), \\ \text{where } Y_m \text{ and } Y_a \text{ are maximum and actual yields, } ET_m \text{ is optimal crop} \\ \text{evapotranspiration, and } K_y \text{ is a yield response factor representing effect of a reduction} \\ \text{in } ET_c \text{ on yield losses.} \end{split}$	ET _c (crop evapotranspiration)
Veysi et al. (2020)	$\begin{aligned} \text{NDVI} &= (\rho_{NIR} - \rho_{RED})/(\rho_{NIR} + \rho_{RED}) \text{SAVI} = \frac{(\rho_{NIR} - \rho_{RED})}{(\rho_{NIR} + \rho_{RED} + L)} (1 + L) \text{MSAVI} &= \frac{1}{2} \left[\sqrt{(2\rho_{NIR} + 1)^2 - 8(\rho_{NIR} - \rho_{RED})} \right] \text{NDWI} = (\rho_{NIR} - \rho_{SWIR})/(\rho_{NIR} + \rho_{SWIR}) \text{TVDI} = \\ \frac{(TS_{obs} - TS_{\min})}{(a + bNDVI - TS_{\min})} \text{CWSI} &= (T_S - T_{Cold})/(T_{Hot} - T_{Cold}) \end{aligned}$	TVDI (temperature vegetation dryness index), NDWI (normalized difference water index), SAVI (soil adjusted vegetation index), MSAVI (modified SAVI), NDVI, and CWSI
Patil et al. (2021)	$CWSI = (T_S - T_{Cold})/(T_{Hot} - T_{Cold})$	CWSI
Gonçalves et al. (2022)	SAVI = $\frac{(\rho_{NIR} - \rho_{RED})}{(\rho_{NIR} + \rho_{RED} + L)} (1 + L)$ ETa and geeSEBAL	ETa (actual evapotranspiration), SAVI, and geeSEBAL (Google Earth Engine - Surface Energy Balance Algorithm for Land)
Bispo et al. (2022)	SAVI = $\frac{(\rho_{NIR} - \rho_{RED})}{(\rho_{NIR} + \rho_{RED} + L)} (1 + L)$ and SETMI hybrid model	SAVI, and SETMI (Spatial Evapo-Transpiration Modeling Interface)
Melo et al. (2022)	CWSI = $(T_c - T_{wet})/(T_{dry} - T_{wet})$ where Twet is the leaf temperature without water stress, Tdry is the leaf temperature under water stress, and Tc is the temperature of the leaf representing the canopy.	CWSI
Watanabe et al. (2022)	$CWSI = 1 - E/E_{p}; where, E=transpiration \ rate, Ep = potential \ transpiration, and \\ CWSI = 1 - E_{WS}/E_{C}; where EC \ and EWS \ denote the transpiration \ rates of Control (irrigated) \ and WS (water stressed canopy), respectively.$	CWSI
Alavi et al. (2024)	$\begin{split} & \text{NDVI} = (\rho_{NIR} - \rho_{RED})/(\rho_{NIR} + \rho_{RED}) \text{MSI} = \rho_{SWIR}/\rho_{NIR} \text{EVI} = \\ & \frac{2.5 \ (\rho_{NIR} - \rho_{RED})}{(\rho_{NIR} + 6\rho_{RED} - 7.5\rho_{BLUE} + 1)} \text{GNDVI} = (\rho_{GREEN} - \rho_{RED})/(\rho_{GREEN} + \rho_{RED}) \text{NMDI} = \\ & \frac{\rho_{NIR} - (\rho_{SWIR} - \rho_{SWILE})}{(\rho_{NIR} + (\rho_{SWIR} - \rho_{SWIRZ}))} \text{D1609} = 1 - \text{R} = 1 - \frac{\rho_{SWIR}}{(0.4431\rho_{NIR} + 0.5569\rho_{SWIRZ})} \text{NTR} = (1 - \rho_{NIR})^2/2\rho_{NIR} \text{NIRv} = \rho_{NDVI} \times \rho_{NIR} \text{Brightness} = 0.3029 \ \rho_{BLUE} + 0.2786 \ \rho_{GREEN} + 0.4733 \\ \rho_{RED} + 0.5599 \ \rho_{NIR} + 0.508 \ \rho_{SWIR} + 0.1872\rho_{SWIRZ} \text{Greenness} = -0.2941 \ \rho_{BLUE} - 0.243 \\ \rho_{GREEN} + 0.5424 \ \rho_{RED} + 0.7276 \ \rho_{NIR} + 0.0713 \ \rho_{SWIR} - 0.1608\rho_{SWIRZ} \text{RVI} = \frac{4\sigma_{vh}}{\sigma_{vh}} \\ \text{DPRVIc} = \frac{\sigma_{vh}(\frac{\sigma_{vh}}{\sigma_{vv}} + 3)}{(\frac{\sigma_{vh}}{\sigma_{vv}} + \sigma_{vv}} DPSVI = \frac{\sigma_{vh}[(\sigma_{vv(Max)}\sigma_{vh} - \sigma_{vv}\sigma_{vh} + \sigma_{vh}^2)}{\sigma_{vv}\sqrt{2}} + \\ \frac{(\sigma_{vv(Max)}\sigma_{vv} + \sigma_{vv}\sigma_{vh} - \sigma_{vv}^2)]}{\sigma_{vv}\sqrt{2}} IDPDD = \frac{(\sigma_{vv(Max)} - \sigma_{vv}) + \sigma_{vh}}{\sqrt{2}} \\ VDDPI = \frac{\sigma_{vh} + \sigma_{vv}}{\sigma_{vv}} ETc = \text{Kc} \times \text{ET}_0 \end{split}$	NDVI, MSI (Moisture Stress Index), EVI (Enhanced Vegetation Index), GNDVI (Green NDVI), NMDI (Normalized Multi-Band Drought Index), D1609, NTR (NIR Transformed Reflectance), NIRv (Near-Infrared Reflectance of Vegetation), Brightness, Greenness, RVI (Radar Vegetation Index), DPSVI (Dual-Pol Radar Vegetation Index), DPSVI (Dual-Polarization SAR Vegetation Index), IDPDD (Inverse dual-pol Diagonal Distance), VDDPI (Vertical Dual de-Polarization Index), DPDD (Dual-Pol Diagonal Distance), ETc (crop evapotranspiration)

indices, hyperspectral imaging, satellite and aerial imagery, and chlorophyll-based estimations have been widely applied for LNC evaluation (Table 3). AI-driven decision support systems further enhance these applications by integrating multi-source RS and IoT data to provide actionable insights for managing nitrogen levels and mitigating salinity impacts (Koohi et al., 2023; Cho et al., 2024). Despite these advancements, challenges such as data quality, accessibility for small-scale farmers, and economic feasibility persist, emphasizing the need for scalable and inclusive technological adoption in sugarcane agriculture.

3.1 Water stress assessment

In the earlier studies, Rahman et al. (2004) employed NDVI to identify sugarcane areas and assess crop conditions, considering

factors like leaf water content, nitrogen deficiency, pigments, foliar nutrients, and agronomic parameters. Abdel-Rahman and Ahmed (2008) found that the infrared/red ratio from Landsat TM NIR radiometer, SWIR bands, and the digital multispectral video (DMSV) sensor were effective in detecting water content in sugarcane crops. Detection of water stress, attributed to a reduction in the photosynthesis process, was found to be best achieved at the canopy level using VIS, red edge, and NIR regions (Berni et al., 2009). Brunini and Turco (2016) investigated sugarcane water stress indices in irrigated areas with different exposures and slopes. Their evaluation of daily water stress index and soil water potential revealed variations based on exposure and slope. The water stress index, derived from infrared thermometry, helped determine the optimal timing for irrigating sugarcane crops. Experiments conducted during various growing phases (tillering,

TABLE 2 Vegetation or spectral indices used in the referenced studies for salinity stress assessment.

Author(s)	Expression(s)/indices	Abbreviation & description
Hamzeh et al. (2012)	NDVI = (R800 -R670)/(R800 +R670) NDWI = (R860 -R1240)/(R860 +R1240) SWSI 1 = (R803 - R681)/ $\sqrt{(R905 + R972)}$ SWSI 3 = (R803-R681) / $\sqrt{(R1174 + R972)}$	NDVI (normalized difference vegetation index), NDWI (normalized difference water index), SAVI (Soil-Adjusted Vegetation Index), and SWSI 1 & 3 (Salinity and Water Stress Indices 1 & 3)
Hamzeh et al. (2013)	$NDVI = (R800-R670)/(R800+R670) \\ NDVI_{705} = (R750-R705)/(R750+R705) \\ SR = R750/R705 \\ VOG1 = R740/R720 \\ REP = 700 + 40\{[(R670+R780)/2-R700]/(R740-R700)\} \\ mNDVI_{705} = (R750-R705)/(R750+R705-2R445) \\ mSR_{705} = (R750-R405)/(R750+R705-2R445) \\ mSR_{705} = (R750-R670) - 0.2(R700-R550)] \times (R700/R670) \\ TCARI_{(670,700)} = [(R700-R670) - 0.2(R700-R550)] \times (R700/R670) \\ TCARI_{(670,700)} = 3[(R700-R670) - 0.2(R700-R550)] \times (R700/R670) \\ ARI = (1/R550) - (1/R700) \\ 2R800 + 1 \\ MSAVI = \S \left[\begin{array}{c} \\ \\ \\ \\ \\ \\ \\ \\ \\ \\ \\ \\ \\ \\ \\ \\ \\ \\ \\$	NDVI (normalized difference vegetation index), NDVI ₇₀₅ (Red edge normalized difference vegetation index), SR (Simple ratio), VOG1 (Vogelmann red edge index), REP (Red-edge position), mNDVI ₇₀₅ (Modified red edge normalized difference vegetation index), mSR ₇₀₅ (Modified SR), MCARI _(670,700) , TCARI _(670,700) , ARI (Anthocyanin reflectance index), MSAVI (Modified soil adjusted vegetation index), OSAVI (Optimized soil-adjusted vegetation index), PRI (Photochemical reflectance index), PRI 2 (Photochemical reflectance index 2), CRI (Carotenoid reflectance index), MSI (Moisture stress index), NDII (Normalized difference infrared index), WI (Water index), NDWI (normalized difference water index), NDWI-Hyp (NDWI-hyperion), DSWI-1 (Disease-water stress index 1), SAVI (Soil-Adjusted Vegetation Index), and SWSI 1, 2 & 3 (Salinity and Water Stress Indices 1, 2 & 3)
Hamzeh et al. (2016)	$\begin{array}{l} R_{NIR} \\ NDVI = (R_{NIR} - R_{RED})/(R_{NIR} + R_{RED}) \\ SR = R_{NIR}/R_{RED} \\ SAVI = L(R_{NIR} - R_{RED})/(R_{NIR} + R_{RED} + L) \\ NDWI = (R_{NIR} - R_{1650})/(R_{NIR} + R_{1650}) \\ SWSI 1 = (R803 - R681)/\sqrt{(R905 + R972)} \\ SWSI 2 = (R803 - R681)/\sqrt{(R1326 + R11507)} \\ SWSI 3 = (R803 - R681)/\sqrt{(R1326 + R11507)} \\ SWSI 3 = (R803 - R681)/\sqrt{(R1174 + R972)} \\ SWSI 4 = (R803 - R681)/\sqrt{(R1174 + R972)} \\ SWSI 5 = (R803 - R681)/\sqrt{(R1174 + R972)} \\ SWSI 6 = (R803 - R681)/\sqrt{(R1174 + R972)} \\ SWSI 7 = (R803 - R681)/\sqrt{(R1174 + R972)} \\ SWSI 8 = (R803 - R681)/\sqrt{(R1174 + R972)} \\ SWSI 9 = (R803 - R681)/\sqrt{(R1174 + R972)} \\ SWSI 1 = (R803 - R681)/\sqrt{(R1174 + R972)} \\ SWSI 1 = (R803 - R681)/\sqrt{(R1174 + R972)} \\ SWSI 2 = (R803 - R681)/\sqrt{(R1174 + R972)} \\ SWSI 3 = (R803 - R681)/\sqrt{(R1174 + R972)} \\ SWSI 4 = (R803 - R681)/\sqrt{(R1174 + R972)} \\ SWSI 5 = (R803 - R681)/\sqrt{(R1174 + R972)} \\ SWSI 6 = (R803 - R681)/\sqrt{(R1174 + R972)} \\ SWSI 7 = (R803 - R681)/\sqrt{(R1174 + R972)} \\ SWSI 8 = (R803 - R681)/\sqrt{(R1174 + R972)} \\ SWSI 9 = (R803 - R681)/\sqrt{(R1174 + R972)} \\ SWSI 1 = (R803 - R681)/\sqrt{(R1174 + R972)} \\ SWSI 1 = (R803 - R681)/\sqrt{(R1174 + R972)} \\ SWSI 2 = (R803 - R681)/\sqrt{(R1174 + R972)} \\ SWSI 3 = (R803 - R681)/\sqrt{(R1174 + R972)} \\ SWSI 4 = (R803 - R681)/\sqrt{(R1174 + R972)} \\ SWSI 5 = (R803 - R681)/\sqrt{(R1174 + R972)} \\ SWSI 6 = (R803 - R681)/\sqrt{(R1174 + R972)} \\ SWSI 7 = (R803 - R681)/\sqrt{(R1174 + R972)} \\ SWSI 8 = (R803 - R681)/\sqrt{(R1174 + R972)} \\ SWSI 9 = (R803 - R681)/\sqrt{(R1174 + R972)} \\ SWSI 1 = (R803 - R681)/\sqrt{(R1174 + R972)} \\ SWSI 1 = (R803 - R681)/\sqrt{(R1174 + R972)} \\ SWSI 1 = (R803 - R681)/\sqrt{(R1174 + R972)} \\ SWSI 1 = (R803 - R681)/\sqrt{(R1174 + R972)} \\ SWSI 2 = (R803 - R681)/\sqrt{(R1174 + R972)} \\ SWSI 3 = (R803 - R681)/\sqrt{(R1174 + R972)} \\ SWSI 3 = (R803 - R681)/\sqrt{(R1174 + R972)} \\ SWSI 3 = (R803 - R681)/\sqrt{(R1174 + R972)} \\ SWSI 3 = (R803 - R681)/\sqrt{(R1174 + R972)} \\ SWSI 3 = (R803 - R681)/\sqrt{(R1174 + R972)} \\ SWSI 3 = (R803 - R681)/\sqrt{(R1174 + R972)} \\ SWSI 3 = (R803 - R681)/\sqrt{(R1174 + R972)} \\ SWSI 3 = (R803 - R681)/\sqrt{(R1174 + R972)} \\ $	R _{NIR} , NDVI (normalized difference vegetation index), SR (Simple ratio), SAVI (Soil-Adjusted Vegetation Index), NDWI (normalized difference water index), SWSI 1, 2 & 3 (Salinity and Water Stress Indices 1, 2 & 3), and SWSI-L (Salinity and Water stress Index- Landsat)

growth, and maturation) on surfaces with slopes ranging from 0 to 40% and different solar exposures indicated that the ideal irrigation timing varied between 2.0 to 5.0 °C, depending on the sugarcane phase. A review by Katsoulas et al. (2016) focused on crop water stress and nutrient detection using reflectance measurement approaches and sensors in a greenhouse. They observed that ground-based sensor data indices were efficient for water stress detection but were influenced by factors such as leaf age, thickness, soil background, and canopy structure. Veysi et al. (2017) introduced a novel method for computing Crop Water Stress Index (CWSI) from satellite data, utilizing hot and cold pixels without the need for ground ancillary data. The study focused on irrigation scheduling in sugarcane during the growing season (May-September) and demonstrated superior performance compared to two alternative approaches, showing a strong coefficient of determination. The researchers observed a negative correlation between Vegetation Water Content (VWC) and CWSI, with R² values ranging from 0.42 to 0.78. Validation of the new approach involved the analysis of eight Landsat 8 satellite images alongside ground truth data obtained through *in situ* measurements of canopy temperature and VWC.

An in-depth analysis of the studies in Table 4 reveals the progressive evolution of crop water stress assessment methodologies, integrating diverse data sources, modelling frameworks, and RS techniques. Early efforts, such as by Hellegers et al. (2009) and Singels et al. (2010), employed models like Surface Energy Balance Algorithm for Land (SEBAL) and CANEGRO for estimating ET and simulating physiological responses under stress, although they faced limitations in replicating yield-related processes. As studies progressed, RS technologies became central, with Teixeira et al. (2016) and Veysi et al. (2017, 2020) combining MODIS, Landsat, and SEBAL with meteorological and soil data, enabling improved spatial and temporal resolution in ET and water productivity estimates. Thermal-based indices, particularly the CWSI, emerged as powerful indicators in studies like Lebourgeois et al. (2010) and Farsi et al., demonstrating strong correlation with

TABLE 3 Vegetation or spectral indices used in the referenced studies for nitrogen levels evaluation.

Author(s)	Expression(s)/indices	Abbreviation & description
Mokhele and Ahmed (2010)	RVI = (R810/R560) PRI = (R531-R570)/(R531+R570) PSRI = (R680-R500)/R750 mSR = (R750-R445)/(R705-R445) REI = R740/R720 CI = R760/R695 NPCI = (R680-R430)/(R680+R430) GMI = R750/R700 ND = (R1075-R730)/(R1075+R730) NDNRI = (R1770-R693)/(R1770+R693) NDVI = (R750-R560)/(R750+R560) mNDVI=(R2200-R2025)/(R2200+R2025) SR = D744/D2142 WBI = R970/R900 WBR = R960/R930 D730, D740, D744	RVI (Ratio Vegetation Index), PRI (Photochemical Reflectance Index), PSRI (Plant Senescence Reflectance Index), mSR (Modified Spectral Ratio), REI (Red-Edge Index), CI (Carter Index), NPCI (Normalized Pigment Chlorophyll Index), GMI (Gitelson & Merzylak Index), ND (Normalized Difference), NDNRI (Normalized Difference Nitrogen Reflectance Index), NDVI (Normalized Difference Vegetation Index), mNDVI (Modified NDVI), SR (Spectral Ratio -Derivatives), WBI (Water Band Index), WBR (Water Band Ratio), and First derivatives at 730, 740, 744.
Abdel-Rahman et al. (2010)	SR _(743, 1316) = R743/R1316 SR _(743, 1317) = R743/R1317 SR _(741, 1323) = R741/R1323	SR (simple ratio)
Abdel-Rahman et al. (2013)	NDVI (691, 2042) NDVI (2042, 691) NDVI (691, 1588) NDVI (518, 1710) NDVI (518, 1710) NDVI (518, 478) NDVI (518, 1578) NDVI (691, 1710) NDVI (1730, 691) NDVI (691, 1699) NDVI (1710, 518) NDVI (1710, 518) NDVI (1578, 518) NDVI (1588, 691) NDVI (2042, 518) NDVI (2042, 518) NDVI (691, 1730) NDVI (691, 478) NDVI (518, 1588) NDVI (691, 478) NDVI (691, 518) NDVI (1730, 691) NDVI (691, 518) NDVI (478, 1699) NDVI (1578, 691)	NDVI (Normalized Difference Vegetation Index)
Soltanikazemi et al. (2022)	$\begin{split} &\text{NDVI} = (\text{NIR}_{842} - \text{RED}_{665}) / (\text{NIR}_{842} - \text{RED}_{665}) \\ &= (\text{B8-B4}) / (\text{B8+B4}) \\ &\text{GEMI} = \left[\text{n} (1 - 0.25 \text{n}) - \frac{\text{B4} - 0.125}{1 - \text{B4}} \right] = \frac{2 \times \text{B8}^2 - \text{B4}^2 + 1.5 \text{B8} + 0.5 \text{B4}}{\text{B8} - \text{B4} + 0.5} \\ &\text{NDI45} = (\text{RED}_{705} - \text{RED}_{665}) / (\text{RED}_{705} - \text{RED}_{665}) \\ &= (\text{B5} - \text{B4}) / (\text{B5} + \text{B4}) \\ &\text{MTCI} = (\text{NIR}_{740} - \text{RED}_{705}) / (\text{NIR}_{740} - \text{RED}_{705}) \\ &= (\text{B6} - \text{B5}) / (\text{B5} - \text{B4}) \\ &\text{IRECI} = (\text{NIR}_{783} - \text{RED}_{665}) / (\text{NIR}_{705} / \text{NIR}_{740}) \\ &= (\text{B7} - \text{B4}) / (\text{B5} / \text{B6}) \\ &\text{GNDVI} = (\text{NIR}_{783} - \text{RG}_{560}) / (\text{NIR}_{783} + \text{G}_{560}) \\ &= (\text{B7} - \text{B3}) / (\text{B7} + \text{B3}) \\ &\text{PSSRa} = \text{NIR}_{783} / \text{RED}_{665} = \text{B7} / \text{B4} \\ &\text{S2REP} = 705 + 35 \times \left[\frac{(\text{NIR}_{783} + \text{RED}_{665} / 2) - \text{RED}_{705}}{\text{NIR}_{740} - \text{RED}_{705}} \right] = 705 + 35 \times \left[\frac{(\text{RF} + \text{B4}) / \text{BF}_{740} - \text{RED}_{705}}{\text{NIR}_{740} - \text{RED}_{705}} \right] \\ &\text{Clgreen} = \text{NIR}_{783} / (\text{GREEN}_{560} = (\text{B8} / \text{B3}) - 1 \\ &\text{Clred-edge} = \text{NIR}_{783} / (\text{RED} - \text{EDG}_{705}) = (\text{B8} / \text{B5}) - 1 \\ \end{aligned}$	NDVI (Normalized Difference Vegetation Index), GEMI (Global Environmental Monitoring Index), NDI45 (Normalized Difference Index 45), MTCI (Meris Terrestrial Chlorophyll Index), IRECI (Inverted Red-Edge Chlorophyll Index), GNDVI (Green NDVI), PSSRa (Pigment specific simple ratio), S2REP (Sentinel-2 Red-Edge Position Index), Clgreen (Chlorophyll green index), and Clred-edge (Chlorophyll Red-edge)

(Continued)

TABLE 3 Continued

Author(s)	Expression(s)/indices	Abbreviation & description
Martins et al. (2024)	Bni = (R750-R500)/(R705-R500) GMi1 = R750/R550 GMi2 = R750/R700 GNDVI = (R780-R550)/(R780+R550) mND ₇₀₅ = (R750-R705)/(R750+R705-2R500) MTCI = (R750-R710)/(R710-R680) NDCI = (R762-R527)/(R762+R527) NDRE = (R790-R720)/(R790+R720) PSNDa = (R800-R680)/(R800+R680) PSNDb = (R800-R635)/(R800+R635) PSNDc = (R800-R470)/(R800+R470) RI-1Db = R735/R720 RI-2dB = R738/R720 RI-3dB = R741/R717 RI-half = R747/R708 RNDVI = (R780-R670)/(R780+R670) SR705 = R750/R705 VOGa = R740/R720 VOGb = (R734-R747)/(R715-R726) VOGc = (R734-R747)/(R715-R720)	BNi (Buschman and Nagel index), GMi1 (Gitelson and Merzlyak index-1), GMi2 (Gitelson and Merzlyak index-2), GNDVI (Green normalized difference vegetation index), mND ₇₀₅ (Modified normal difference index), MTCI (MERIS terrestrial chlorophyll index), NDCI (Normalized difference Chlorophyll index), NDRE (Normalized difference red-edge), PSNDa,b,c (Pigment specific Normalized difference a, b, & c), RI-idB (Ratio indice-idB, i=1,2,3), RI-half (Ratio index-Half), RNDVI (Red normalized difference vegetation index), SR ₇₀₅ (Simple ratio 705), VOGa,b,c (Vogelman indice-a, b, & c).

field-based measures of water deficit, despite challenges like cloud interference and calibration complexity. ML and deep learning (DL) significantly enhanced CWS assessment in later studies. For instance, Virnodkar et al. (2021) employed DenseResUNet and achieved high segmentation accuracy for stressed fields, while Alavi et al. (2024) and Melo et al. (2022) showed that advanced ML models like Random Forest and Inception-ResNet-v2 provided highly accurate predictions (R² = 0.92-0.99, RMSE = 2.02-0.32 mmd⁻¹) of crop water demand and thermal stress patterns. Notably, Goncalves et al. (2022) and Bispo et al. (2022) showcased hybrid modeling approaches using Google Earth Engine - Surface Energy Balance Algorithm for Land (geeSEBAL) and Spatial Evapo-Transpiration Modeling Interface (SETMI), integrating RS with in-field micrometeorological data to refine ET estimates and irrigation management (RMSE = 0.46, R² = 0.94 - 0.97). Across studies, spectral indices (e.g., TVDI: temperature vegetation dryness index; NDVI), soil moisture probes, thermal imaging, and energy balance models consistently contributed to assessing water stress, though limitations such as low-resolution meteorological data, cloud cover, and sensor calibration persisted. Collectively, these investigations underline a clear trend toward integrating multisource RS data with AI/ML algorithms, enabling more precise, scalable, and real-time assessments of water stress in sugarcane agriculture supporting smarter irrigation scheduling and resilient crop management.

3.2 Monitoring and estimation of salinity stress

Salinity is a critical factor affecting soil health and crop growth (Chele et al., 2021). Salinity stress assessment in sugarcane fields involves evaluating the effects of salinity on sugarcane growth, physiology, and yield. Various studies have been conducted to assess the impact of salinity stress on sugarcane. Kumar et al.

(2023a) found that salinity stress significantly affected sugarcane yield, commercial cane sugar (CCS) yield, number of millable cane (NMC), single cane weight (SCW), and pol % in juice. Vu et al. (2023) demonstrated that the application of biochar had positive effects on the growth and physiology of sugarcane under both saline and nonsaline conditions. Dhansu et al. (2022) conducted experiments to evaluate the response of popular sub-tropical sugarcane varieties to salinity stress and observed significant reductions in growth, relative water content (RWC), and gas exchange traits under saline conditions. Simoes et al. (2023) evaluated the growth-related traits of Saccharum genotypes under saline and non-saline conditions and identified promising genotypes with enhanced salinity tolerance. Djajadi et al. (2022) investigated the influence of salinity stress on sugarcane growth, soil nutrient content, and leaves and found that saline stress decreased soil organic and available K (Potassium), as well as the content of N and K in sugarcane leaves. Mohanan et al. (2021) also discussed the assessment of salinity stress tolerance in transgenic sugarcane plants overexpressing the Glyoxalase III gene. However, these studies not utilized the AI algorithms and RS data. As per the current advancements, AI algorithms applied to RS data can effectively identify and quantify soil salinity levels.

The combined analysis of studies in Table 5 demonstrates the growing effectiveness of integrating hyperspectral and multispectral RS data with ML algorithms to assess salinity stress in agricultural soils, particularly sugarcane fields. Hamzeh et al. (2012) laid foundational work by applying classifiers like Support Vector Machine (SVM), Spectral Angle Mapper (SAM), Minimum Distance (MD) and Maximum Likelihood algorithm (MLA) on Hyperion imagery in Khuzestan, Iran, where SVM outperformed others with a classification accuracy of 78.7%, revealing that RS-based salinity mapping can support targeted management of sugarcane in varied salinity zones. Building on this, Hamzeh et al. (2013) compared 21 hyperspectral vegetation indices (VIs), identifying optimized indices like OSAVI (Optimized soiladjusted vegetation index) and VOG1 (Vogelmann red edge

TABLE 4 Critical observations from referenced studies for crop water stress assessment.

Studies	Study area and data	Methods used	Results	Remarks
Inman- Bamber (2004)	Kalamia Estate, Ayr, Queensland, Australia. Objectives: validate 50-stalk elongation criterion, study dry matter partitioning. Neutron moisture meter, AWS installed for data collection. Stress tracked via SWD, cumulative ET _o .	Randomized split plot design. Significance of treatment effects determined using TTEST procedure in SYSTAT.	Sugarcane biomass tolerates soil water deficits, affecting dry matter partitioning. Stress reduces leaf and stalk elongation, increasing sucrose yield. Senescence reduces green leaf number per stalk. Leaf elongation and appearance are interdependent. Mean leaf extension rate correlated with daily minimum temperature.	Limited understanding: water stress impact on sugar yield and yield-forming processes. Dry matter partitioning response to water deficits unclear. Sugarcane growth models need enhancement.
Hellegers et al. (2009)	South Africa. Landsat image of the Inkomati catchment (Path 168-Row 78). Actual water consumption and associated biomass production using SEBAL.	Crop water productivity (CWP) is analyzed by using Surface Energy Balance Algorithm for Land (SEBAL) and RS. Socio-economic analysis to quantify foregone economic water productivity (EWP).	The results show that diverting water away from crops with low CWP is not always cost-effective in terms of foregone EWP.	Production costs cannot be derived by RS. Not all biomass produced is beneficial biomass. Only the ET from irrigation can be managed by water reallocation.
Teixeira et al. (2016)	Sao Paulo state, Brazil. MODIS images and gridded weather data.	SAFER quantifies ET. Monteith's RUE (Radiation Use Efficiency) model quantifies biomass (BIO). Water productivity (WP) calculates ratio of BIO to ET.	Mean values for ET: 0.6-4.0 mm/day. BIO: 20–200 kg/ha/day. WP: 2.8-6.0 kg/m³. Soil moisture suggests supplementary irrigation during grand growth.	Estimate errors for emissivity in Sao Paulo, Brazil contrasting environmental conditions.
Singels et al. (2010)	Data from two experiments at Mount Edgecombe, South Africa were used: 2002/03 trial monitored WU (Water uptake), CAR, Plant extension (PER) (PER), SA over 40 days, starting with 5-monthold well-watered sugarcane. 1998/99 trial-imposed stress 3 months post-planting.	CANEGRO model calculated root length density. BEWAB WU model recommended over CERES WU. Models simulated water stress impact on sink activity and sucrose accumulation (SA).	Soil water's limiting point differed between Experiment A (0.129) and B (0.307), due to evaporative demand variations. Sink activity responded faster and at higher soil water contents in Experiment B. Severe water stress resulted in the cessation of sucrose accumulation.	Models minimized time gaps between sink and source activity reduction. CANESIM overlooked water stress impact on sink. CANEGRO capped root length density. CANESIM inadequately replicated sucrose accumulation variance under water stress.
Lebourgeois et al. (2010)	Southern Reunion Island. Thermal data from clear days and 1-hour afternoon in 2007 set empirical CWSIe baselines. 2008 data tested method's robustness.	Empirical CWSIe method, Water Deficit Index method. Theoretical method (CWSIt), and Diurnal study method.	AET/MET vs. (1 - CWSIe) regression (0.4–1 range) showed significant correlation (global $R^2 = 0.75$, RMSE = 0.12), indicating CWSIe's efficacy even in humid conditions [vapor pressure deficit (VPD) 0.5-2.1].	CWSIt not for irrigation scheduling. Unsuitable for early season. No canopy temperature for irrigation calculation.
Brunini and Turco (2016)	Jaboticabal, SP, Brazil. Experiment used weather station data. Soil samples monitored moisture. Tensiometers measured water potential. Irrigation based on ET.	Experimental area assessed various surfaces. Daily water stress index and soil water potential evaluated. Drip irrigation employed. Temperature readings taken. Water stress index calculated. Analysis done via ANOVA and Tukey test.	Sugarcane water stress varies with terrain exposure and slope while areas with water stress index was above 5.0 °C had lower yield values. Lack of water affects tillering. Complementary irrigation mitigates yield reduction.	Rainfall limited in initial sugarcane growth months. 2013–14 water stress damaged crop severely. Yield affected by low rainfall, high temperatures.
Veysi et al. (2017)	Salman Farsi Agro industry, Iran. Dataset: canopy temperature, eight Landsat 8 images. Regression set temperature, VPD lower boundary. Three water stress index methods analyzed.	Empirical CWSI, Idso method with handheld IR thermometer, and Landsat 8 thermal data. New satellite CWSI retrieval proposed. Hot and cold pixel method used.	Strong correlation: field-based and satellite-derived CWSI. Negative VWC-CWSI relationship (R ² : 0.42–0.78). Water stress categorized: high, medium, low. Proposed CWSI approach aids irrigation scheduling in sugarcane.	Challenges in field temperature measurement. Key calculations establish temperature bounds. Requires additional data and complex computations.
Singels et al. (2018)	Mpumalanga, South Africa. RS data (2011-2013) via SEBAL. Ground FPAR and biomass estimates. ET measured using surface renewal system. Meteorological data from National Oceanic and Atmospheric Administration (NOAA) database. Soil water	RS estimates ET, biomass via SEBAL. Ground FPAR, biomass measures. Surface renewal (SR) system estimates ET. Kc values calculated from ET, grass evaporation. Comparison with field data. Soil water monitored. drought stress index (DSI) and waterlogged stress index (WLI) computed. Thresholds calibrated using SEBAL. Meteorological data for Penman-Monteith ET.	RS FPAR, biomass correlate strongly with field ($R^2=0.89,0.78$). SEBAL ET surpasses SR by 5mm/week. SEBAL Kc values aligns better with literature.	32% fields below economic thresholds. SEBAL shows lower ET without sufficient soil water. SEBAL biomass production (TDM) should exceed aboveground dry biomass (ADM). SR estimates ET via energy balance equation.

(Continued)

TABLE 4 Continued

Studies	Study area and data	Methods used	Results	Remarks
	monitored with Aquacheck probes.			
Picoli et al. (2019)	Northwest São Paulo State, Brazil. Landsat detects sugarcane drought. Spectral indices from Red, NIR, SWIR bands. Climatological soil- water balance (CSWB) model predicts water status. European Centre for Medium-Range Weather Forecasts (ECMWF) provides meteorological data.	Assessing plant-sensitive spectral indices. Comparing with CSWB-estimated soil moisture. Developing new indices combining NIR, SWIR. Using cluster, discriminant analysis for drought detection and monitoring.	New indices for sugarcane drought via Landsat. Spectral indices correlate with water balance. 65% accuracy drought system via cluster analysis. Discriminant analysis optimal for drought monitoring.	CSWB serves as benchmark, but prone to errors. Future studies prioritize fewer indices, local variables, especially during phenological phases. Caution against low- resolution meteorological data like ECMWF.
Waqas et al. (2019)	Command area of 3 distributaries, namely Killianwala, Mungi and Khurrianwala lying in the district of Faisalabad, Pakistan. Multispectral images of LANDSAT-7 were used for study.	NDVI classification, accuracy assessed. ET by Penman-Monteith equation. Crop water via 10-day Kc value, irrigation demand from LULC.	LULC mapping for three distributaries. Accuracy: 84% and 86%. Estimation of crop water requirement, irrigation demand. Canal water deficit (CWD) calculated.	Comparatively satisfactory results were noticed.
Pereira et al. (2020)	Central Goiás, Brazil. Leaf temperature (TL and land surface temperature (TS) measurements. Landsat 8 imagery. Weather data, rainfall. Bands 10, 11 for NDVI.	TL by IR thermometer, TS viaLandsat8.Waterbalance detects water deficit (WD) and surplus (WS). T _L -T _a , T _S -T _a calculated. Bands 10, 11 for temperature. Emissiv itycalibratedwithsoil cover factor (SCF).	TL detects WD, WS in sugarcane. TS has limited in WD detection. At band 11, TS tends to smaller. Calibration uncertainty mainly with band 11.	TS needs improvement based on surface properties. T _L -T _a error at 20% for some dates. Band 11 calibration was uncertain. Further investigation needed.
Triadi et al. (2020)	Sugarcane plantation in Djengkol, Kediri, East Java. Secondary data from various sources, Oct 2017-Sep 2019. Landsat 8, MODIS-Aqua satellite data for water vapour.	CWSI, NDVI, Split-window algorithm to calculate CWSI by analysing drought stress response from land surface temperature (LST).	CWSI and NDVI can effectively estimate the level of water stress in sugarcane. The results can be useful for irrigation management in sugarcane fields.	CWSI is very sensitive to cloud cover. The water vapor data used has a very large resolution so it tends to be inaccurate.
Virnodkar et al. (2020)	Not explicitly mentioned the specific dataset used.	RS and ML methods, coupled with canopy temperature-based spectral indices, alongside various techniques such as IR thermometry, stomatal conductance and stem water potential measurements.	Review on ML techniques and RS have been used for CWS assessment in various crops including sugarcane. ML and RS can be used to improve water management and irrigation practices in agriculture.	Existing methods for evaluating water stress can be greatly improved. CWS assessments require attention from the research community.
Das et al. (2020)	Northeast Thailand. Dataset: Kc, Leaf Area Index (LAI), yield data. Split into training/ testing sets. Linear, polynomial regression for prediction.	RS observation with ML and land surface model (LSM). Regression and polynomial models established for LAI vs Kc and found $6^{\rm th}$ order polynomial is accurate with adjusted $R^2=0.87$, RMSE = 0.089, MAPE = 8.63. Highresolution LSM computes daily ET. Yield response was analyzed in 19 fields.	Initial and early stages have minimal ETc distribution, contrasting with higher levels during grand growth and yield formation. Spatiotemporal disparities noted across fields. Comprehensive analysis affirms yield-water consumption correlation.	Limited field scale studies on actual water consumption of sugarcane. Uncertainty in yield due to various factors. Dependence on optimal conditions for maximum yield and ET.
Veysi et al. (2020)	Sugarcane farms of Salman Farsi. Salman Farsi, southwest of Iran. Landsat 8 satellite images.	Field measurements of soil moisture and canopy temperature, alongside calculated indices using optical and thermal IR wavelengths, to analyze their relationship with soil moisture.	Both CWSI and temperature vegetation dryness index (TVDI) align in assessing soil moisture, implying their suitability for irrigation scheduling. TVDI shows stronger correlation $0.35 \le R^2 \le 0.66$ and spatial consistency with soil moisture. RMSE was less than 0.2. Comparison between recorded irrigation and soil moisture levels in the farms revealed three distinct classes.	Vegetation indices based on optical bands do not show a good coefficient of determination R ² .

(Continued)

TABLE 4 Continued

Studies	Study area and data	Methods used	Results	Remarks
Patil et al. (2021)	Area not specified. Landsat 8 satellite image.	In R, METRIC-based water package computes broadband albedo, LAI, Land surface temperature (Ts), long-wave radiation, Rn, incoming solar radiation, and top-of-atmosphere (TOA) reflectance.	The comparative results indicate that both the results are 91% alike. The comparison of ET and CWSI indicated that both CWSI and ET maps can be used for the assessment of crop water status and irrigation scheduling.	Further works should consider the influence of cultivation methods, climate conditions and other factors affecting CWSI.
Virnodkar et al. (2021)	A dataset containing water- stressed sugarcane crops from four talukas (Gokak, Raibag, Jamkhandi, and Mudhol) in Karnataka, India. Cloud-free Sentinel-2 satellite images.	Encoder-decoder architecture with UNet, SegNet, and FCN models. DenseNet architecture with densely connected layers. Semantic segmentation using deep learning (DL) techniques.	The 'DenseResUNet' model achieves robust performance, with 61.91% mean Intersection over Union (mIoU) and 80.53% accuracy in segmenting waterstressed sugarcane fields, outperforming UNet, ResUNet, and DenseUNet with scores of 32.20%, 58.34%, and 53.15%, respectively.	Results highlight semantic segmentation for CWS detection with limited RS data. Increasing training samples could improve accuracy.
Gonçalves et al. (2022)	24 ha commercial field in western Sao Paulo, Brazil. Landsat 8 Operational Land Imager (OLI) and Thermal Infrared Sensor (TIRS), Landsat 7 Enhanced Thematic Mapper Plus (ETM), ERA5-Land reanalysis dataset, Shuttle Radar Topography Mission (SRTM) digital elevation data.	RS method estimates actual evapotranspiration (ETa). Google Earth Engine (GEE)-Surface Energy Balance Algorithm for Land (geeSEBAL) used. Calibration with Inverse Modeling at Extreme Conditions (CIMEC). Comparison with eddy covariance (EC) data. RS-based soil water balance for water stress. Statistical analysis includes R ² , RMSE, and Bias.	geeSEBAL accurately estimated sugarcane ETa (RMSE = 0.46 , R^2 = 0.97) in Brazil, matching EC data, standard values, and flux tower data. It identified water stress, aiding irrigation management.	Soil heat flux (W/m2) values have little influence on energy balance (EB) due to their low values. Soil-adjusted vegetation index (SAVI) values decrease during the maturation stage of sugarcane. Limited availability of climate data in certain areas.
Bispo et al. (2022)	Field data from EC system in Andradina, São Paulo. Meteorological data from Itapura station. RS data used for Spatial EvapoTranspiration Modeling Interface (SETMI) model. Spectral reflectance informs Kcbrf relationship. SCS Runoff equation for effective precipitation.	Eddy covariance tower for micrometeorological variables. RS method for ETa. Two-source energy balance model (TSEB) and RS-water balance (RSWB) coupling. Hybrid model SETMI. Basal Kc from SAVI. Bowen Ratio adjusts latent heat flux (IE) and sensitive heat flux (H). IE converted for ETa. Reference evapotranspiration (ETo) from FAO-56. Water use optimization for sugarcane.	Energy balance components correlated strongly with EC data (ET R ² = 0.94, Correlation coefficient=0.88). Model linked SAVI to sugarcane's crop coefficient (Kcb). Average Kcb: 0.73 for 4th ratoon, 0.70 for 5th. Maximum Kcb about 1.23. ETa averaged 1025 mm, with daily rates of 2.9 mm. SETMI model enhanced irrigation management.	Much significant results were observed.
Melo et al. (2022)	University of Sao Paulo, Brazil. Inception-Resnet-v2 pretrained on ImageNet (10 million images, 10,000 categories). Model trained on 1.2 million images. Validation: 1008 images.	Inception-Resnet-v2 neural network model evaluated thermal sugarcane images, outperforming traditional methods in water stress assessment accuracy.	Inception-Resnet-2 surpassed human assessments, showing 23%, 17%, and 14% higher accuracy in detecting thermal stress across soil available water capacity (AWC) classes of 25%, 50%, and 100%, respectively.	No strong limitations were noticed.
Watanabe et al. (2022)	University of Ryukyus greenhouse, Okinawa, Japan: Monitored canopy temperature (CT) under control and water stress, along with photosynthesis, CWSI, and thermal images' RGB channels. Recorded gray levels for both conditions.	Temperature measured by thermal camera and infrared thermometer. Mean CT values for control and water-stressed canopies analyzed statistically in R. Correlation assessed.	Thermal images can distinguish between well-watered and water-stressed canopies. CT measurement and thermography are both useful for water stress detection. R gray level is a good indicator of sugarcane water status. CWSI is correlated with differences in CT and R gray level.	CT readings may be influenced by weather conditions. Comparing CT readings may not be reliable in bad weather. Thermal images may more accurately reflect changes in CT.
Alavi et al. (2024)	Khuzestan province, southwest of Iran. Multisource RS data. Meteorological and ground measurements (Meteo-GM). Sentinel-1 Synthetic Aperture Radar (SAR) data.	4 most popular tree-based ML algorithms, namely M5-pruned (M5P), random forest regression (RFR), gradient-boosted regression trees (GBRT) and extreme gradient boosting (XGBoost).	The RFR algorithm yielded the most accurate ETc estimates, followed by XGBoost, GBRT, and M5P algorithms ($R^2 = 0.92-0.99$, RMSE = $2.02-0.32$ mmd ⁻¹). Meteo-GM models improved with optical, thermal infrared (TIR), and SAR RS data ($R^2 = 0.99$, RMSE = 0.32 mmd ⁻¹ for TIR, $R^2 = 0.98$, RMSE = 0.65 mmd ⁻¹ for SAR). Sobol's sensitivity analysis identified key input variables for ETc estimation.	Optical RS methods have limitations in assessing crop water requirements. Hybrid approaches combining thermal and optical information are needed. Cloud cover restricts the application of optical sensors. Reliance on radar sensing, specifically Sentinel-1 SAR, for continuous observation.

TABLE 5 Critical observations from referenced studies for salinity stress estimation.

Studies	Study area and data	Methods used	Results	Remarks
Hamzeh et al. (2012)	Hakim Farabi Farming and Industrial Lands, Khuzestan, Iran, spanning 774 km ² . Field data collected in Sep 2010 at 191 locations, sampling soil (0–45 cm) salinity levels ranging from 1.5 to 9.7 dSm ⁻¹ . Modeling used 125 samples, validation 66. Hyperion image classified with various classifiers.	Support Vector Machine (SVM), Spectral Angle Mapper (SAM), Minimum Distance (MD) and Maximum Likelihood algorithm (MLA).	SVM classifier or PCA (1-5) achieved the highest accuracy (78.7%) and kappa coefficient (0.68) in salinity stress classification. Salinity maps aid agricultural management, indicating low, moderate, and high salinity areas affecting crop yield.	SAM classifier accuracy depends on endmember selection. ML needs adequate training data for covariance. Limited datasets vs. bands.
Hamzeh et al. (2013)	Khuzestan, Iran, 774 km² area. Soil salinity measured at 108 sugarcane points, 60 for modeling, 48 for validation. Hyperion image acquired Sep 2, 2010.	Hyperspectral VIs evaluated for soil salinity estimation included 21 existing VIs and newly developed ones, such as optimized SAVI and Vogelmann red edge.	SWSI-3, SWSI-1, VOG1, SWSI-2 optimal for salinity, RMSE 1.14-1.17 dSm $^{-1}$. Chlorophyll/ water bands effective. OSAVI (R 2 = 0.69), chlorophyll/NIR indices correlate strongly.	Hyperspectral RS vital for precision. Satellite data limited. PRI effectiveness varies with crop type, growth stage. Pigment-related indices weaken season-end.
Hamzeh et al. (2016)	Khuzestan, Iran. Sep 2010 field data: 25 fields, 0–45 cm depth, 191 samples with varied salinity. Modeling: 125; validation: 66.	SVM, SAM, MD, MLA.	Landsat excelled in categorical salinity stress classification (84.84% accuracy, Kappa 0.77), while Hyperion outperformed in quantitative estimation. Salinity and Water Stress Index (SWSI) demonstrated superior prediction for salinity stress, favoring Landsat for categorical mapping.	Confusion between low/ moderate and moderate/ high salinity classes. Indirect assessment is costly. <i>In situ</i> accuracy relies on ground data density/distribution.
Haq et al. (2023)	Landsat 8 data for spectral analysis. Fifty-five soil samples from field survey of Kot Addu, Pakistan.	RFR, SVM	RFR achieved R ² of 0.94 using Differential Vegetation Index (DVI).	Efficient method for assessing soil salinity at local scales.
Kaplan et al. (2023).	393 soil samples drawn in United Arab Emirates. Sentinel-2 satellite imagery for RS data.	RF, SVM	Strong correlation (0.84) between modelling and test results.	Interesting findings for future studies at other sites.

index) as reliable predictors of soil salinity with strong correlations (R² up to 0.69), underscoring the importance of selecting appropriate spectral bands sensitive to chlorophyll and water content. Hamzeh et al. (2016) further contrasted Hyperion and Landsat data, concluding that while Landsat delivered superior categorical classification accuracy (84.84%, Kappa 0.77), Hyperion was better suited for continuous salinity estimation. Notably, their findings introduced the Salinity and Water Stress Index (SWSI) as a robust metric for predicting salinity levels. Recent studies shifted toward advanced ML approaches for broader applicability. Haq et al. (2023) and Kaplan et al. (2023) demonstrated that ensemble learning methods such as RF Regression (RFR) and SVM using Landsat 8 and Sentinel-2 data respectively, achieved high accuracy in salinity prediction ($R^2 = 0.94$ and 0.84), confirming the scalability of RS-ML integration for local to regional salinity monitoring. Overall, the comparative findings highlight a consensus that hyperspectral data combined with tree-based ML models yield reliable predictions of salinity stress, with vegetation indices and spectral reflectance offering crucial insight. However, accuracy is often limited by sensor resolution, endmember variability, and the spatial distribution of ground truth data. Accurate yield predictions based on salinity levels can also help optimize resource allocation and improve overall crop management strategies, potentially increasing sugarcane yield and quality (Waters et al., 2025). These studies collectively highlight the value of tailored RS-ML frameworks in salinity stress management, enabling precision interventions in salt-affected sugarcane agroecosystems.

3.3 Estimation of nitrogen levels

Reckoning leaf N using RS in sugarcane crops is important for optimizing nitrogen fertilizer management and improving crop growth and yield (Reyes-Trujillo et al., 2021). In recent years, different algorithms have been developed to combine spectral reflectance features with ML techniques for the estimation of leaf physiological parameters, including chlorophyll content, moisture content, and nitrogen content (Gai et al., 2023). RS techniques, such as digital image processing, hyperspectral data analysis, and drone multispectral imaging, can provide valuable information on leaf N concentrations and crop vigor. These techniques allow for nondestructive and fast estimation of nitrogen levels, enabling more precise and efficient fertilizer application (Lofton, 2012; Barros et al., 2021). By analyzing the correlation between LNC and various image features, regression models can be constructed to accurately estimate nitrogen content based on color and texture parameters (Li et al., 2022). Additionally, RS can help determine the optimum nitrogen rate and application timing for sugarcane production, ensuring that nitrogen is applied at the right time and in the right amount to maximize crop yield (Abebe et al., 2023).

The studies summarized in Table 6 emphasize the growing reliance on hyperspectral and multispectral RS combined with ML models for estimating nitrogen (N) content in sugarcane crops. Ahmed (2010) used hyperspectral RS in shade house trials to assess the impact of nitrogen and silicon treatments, identifying correlations between red-edge indices (e.g., R740/R720) and N

TABLE 6 Critical observations from referenced studies for nitrogen content evaluation.

Studies	Study area and data	Methods used	Results	Remarks
Ahmed (2010)	South African Sugarcane Research Institute (SASRI), South Africa, conducts N × Si × variety trials in shade houses to study stalk borer (Eldana saccharina) infestation.	Hyperspectral RS and ANOVA analyzed for significant reflectance differences due to N and Si (Silicon) treatments at each wave length across cane ages.	Red-edge (R740/R720) correlates with N concentration. NDVI (R750-R560)/(R750+R560) with Si concentration. ND (R1075-R730)/(R1075+R730) with N: Si ratio. N treatment influences 400–740 nm reflectance (p< 0.05) on 10-month cane.	High RMSE in N and Si regression models. Weak leaf reflectance-biochemical correlations. Spectral data from one leaf, chemical analysis from three leaves.
Abdel- Rahman et al. (2010)	Umfolozi mill supply area in KwaZulu-Natal (KZN) Province, South Africa. <i>In situ</i> spectroscopic data of sugarcane leaf samples.	First-order derivative spectra. Calculation of slope of the spectrum. Locating positions of absorption features and inflection points.	R743/R1316 ratio VI from reflectance's first-order derivatives had highest $R^2 = 0.76$ correlation with sugarcane leaf N concentration.	Need to explore the usefulness of <i>in situ</i> spectroscopy at canopy level using handheld, airborne and spaceborne sensors.
Abdel- Rahman et al. (2013)	KwaZulu-Natal Province, South Africa. 163 out of 196 calibrated wavebands were used in this study.	RF analyzes hyperspectral data, predicts sugarcane N concentration using RF regression. Forward selection identifies crucial vegetation indices; RFs iteratively fit for index inclusion.	RF and Stepwise multiple linear (SML) regression models predict sugarcane N concentration well (RF: $R^2 = 0.67$, RMSEV = 0.15%; SML: $R^2 = 0.71$, RMSEV = 0.19%). RF shows promise with hyperspectral data.	Excluded spectral regions with strong water absorption. Used 163 of 196 wavebands. The method may not suit low-N sites, or small-scale farms due to spatial resolution limitations.
Soltanikazemi et al. (2022)	Amir Kabir Sugarcane Agro- industry located in Ahvaz city, Khuzestan province, Iran. Sentinel-2 data.	RF model, and SVR model. NDVI, GEMI, MTCI, S2REP, PSSRa, NDI45, IRECI, GNDVI, Clgreen, and Clred- edge indices were calculated using QGIS software.	R ² for RF and SVR were 0.59 and 0.58, respectively, and the corresponding RMSE was 0.08 and 0.09, respectively.	RF better than SVR for N yield estimation. More ground data allows diverse DL model application. Multi-temporal data enhances results.
Martins et al. (2024)	Jau, Piracicaba, Santa Maria da Serra. Data from the variety SP 81 3250, cultivated in three experimental areas.	Obtained spectral curve, applied vegetation indices. Lab analyzed plant tissues for Total Foliage Nitrogen (TFN). Model predicted sugarcane N.	Top indices: BNi ($R^2 > 0.66$, RMSE< 3.50 g/kg), GNDVI ($R^2 > 0.65$, RMSE< 3.67 g/kg), NDRE ($R^2 > 0.68$, RMSE< 3.18 g/kg), RI-1db ($R^2 > 0.69$, RMSE< 3.66 g/kg), VOGa ($R^2 > 0.69$, RMSE< 3.44 g/kg). SP813250 variety's predictive potential reduced up to 50% in R^2 , in some cases due to environmental factors.	Reflectance varies in same variety across soils. Model instability across harvests. High noise in blue wavelengths of spectral curves.

levels. However, the study faced limitations such as weak reflectance-biochemical correlations and inconsistency between spectral and chemical sampling methods. Abdel-Rahman et al. (2010) advanced the analysis by using first-order derivative spectra to identify sensitive wavelengths, achieving an R² of 0.76 with the R743/R1316 ratio, yet noted the need for scalability to canopy-level applications. Expanding the scope, Abdel-Rahman et al. (2013) evaluated 163 hyperspectral bands using RF and stepwise multiple linear (SML) regression models, both yielding reliable predictions (RF: $R^2 = 0.67$, RMSEV = 0.15%; SML: $R^2 = 0.71$, RMSEV = 0.19%), demonstrating the potential of hyperspectral data for accurate N monitoring. In a more recent study, Soltanikazemi et al. (2022) utilized Sentinel-2 imagery and calculated multiple vegetation indices (e.g., S2REP, IRECI: Inverted Red-Edge Chlorophyll Index, NDVI) using RF and SVR, achieving modest performance ($R^2 = 0.59$, RMSE = 0.08), with RF slightly outperforming SVR (R² = 0.58, RMSE = 0.09). They emphasized the benefit of larger ground datasets and multitemporal imagery to improve robustness. Finally, Martins et al. (2024) provided a detailed comparison of vegetation indices such as BNi: Buschman and Nagel index, NDRE: Normalized Difference Red-Edge, GNDVI: Green NDVI, and RI-1db: Ratio Index, all yielding R² > 0.65 and RMSE< 3.7 g/kg. However, environmental variability across locations and seasons influenced the predictive capacity of their models, with performance dropping by up to 50% for the same variety (SP 81 3250). Together, these studies indicate that while RS-based N estimation in sugarcane is promising, particularly with indices targeting red-edge and near-infrared regions, the accuracy is influenced by factors like sensor resolution, environmental heterogeneity, sample consistency, and model type. The integration of ML, especially ensemble models like RF, enhances predictive reliability, but operational deployment still requires more stable, scalable, and temporally adaptive frameworks for practical field use.

3.4 Software application

This review systematically examined all the referenced studies to identify the use of specific statistical software, programming languages, or analytical tools for implementing AI-RS methodologies related to the estimation of water stress, salinity stress, and LNC in sugarcane farming. Six studies explicitly mentioned the use of software or coding frameworks. These include SYSTAT (Inman-Bamber, 2004), QGIS Desktop (Triadi et al., 2020), R, Python, and MATLAB (Virnodkar et al., 2020;

2021), R and MATLAB (Watanabe et al., 2022), Microsoft Excel 2019 and Python's Scikit-learn library (Gai et al., 2023), and Environment for Visualizing Imagery (ENVI) 5.3.1 for image visualization and analysis (Alavi et al., 2024). Although many studies reported the application of RS and ML methods, only a few provided explicit details of the software environments or coding frameworks used.

3.5 Recommendations: best solutions from referenced studies

A critical synthesis of previous research (1981–2025) highlights several methodological approaches that stand out as best-practice solutions for stress detection in sugarcane agriculture. Thermal and hyperspectral remote sensing combined with energy balance models, such as SEBAL and CWSI, have provided reliable estimates of evapotranspiration and crop water stress, especially when integrated with meteorological and soil data to support irrigation scheduling (Hellegers et al., 2009; Veysi et al., 2017; Teixeira et al., 2016; Gonçalves et al., 2022). Recent advances demonstrate that deep learning models, including DenseResUNet and Inception-ResNet-v2, applied to high-resolution Sentinel-2 and UAV imagery, significantly improve canopy-level water stress segmentation and thermal pattern prediction (Virnodkar et al., 2021; Alavi et al., 2024; Melo et al., 2022). For salinity stress assessment, the combination of hyperspectral imagery with SVM classifiers and tree-based ensemble methods such as RFR has consistently yielded high classification accuracy and predictive performance across diverse environments (Hamzeh et al., 2012, 2013; Haq et al., 2023; Kaplan et al., 2023). Similarly, for nitrogen estimation, red-edge and NIR vegetation indices integrated with RF or SVR have shown strong correlations with leaf nitrogen content, offering scalable and non-destructive nutrient monitoring solutions (Abdel-Rahman et al., 2010, 2013; Soltanikazemi et al., 2022; Martins et al., 2024). In addition, data fusion approaches and cloud-based platforms like Google Earth Engine have enabled the integration of multi-sensor datasets, improving spatiotemporal resolution and analytical efficiency (Gonçalves et al., 2022; Bispo et al., 2022). Jointly, these approaches represent the most effective, validated solutions for operationalizing AI-RS frameworks in precision water, salinity, and nutrient management for sugarcane.

4 Challenges and limitations

Despite significant advancements, several challenges and limitations persist in the application of RS and AI technologies for assessing water stress, salinity stress, and LNC in sugarcane crops. These challenges primarily arise from the complexity of environmental conditions, limitations in sensor technology, data processing requirements, and the need for robust model calibration and validation.

4.1 Technical and sensor limitations

Spatial resolution remains a major constraint, as RS instruments often struggle to capture detailed information at the individual plant or plot level in large sugarcane plantations. Similarly, limited temporal resolution hampers the ability to monitor short-term fluctuations in water stress, salinity, and nutrient dynamics, which are critical for understanding crop responses across growth stages. While hyperspectral sensors can provide improved spectral resolution, they often face limitations in spatial coverage, data volume, and operational costs. Low radiometric sensitivity (radiometric resolution) can also limit the detection of subtle crop stress signals, especially in early stages. Cloud cover further complicates consistent monitoring by obstructing satellite imagery, particularly in regions prone to frequent cloudiness. In addition, high-quality RS data from advanced sensors can be expensive and less accessible, restricting adoption among resource-limited farmers and researchers.

4.2 Environmental and field variability

Variations in soil type, crop age, plant density, and microclimatic conditions significantly influence spectral reflectance, complicating the accurate discrimination of stress signals (Waters et al., 2025). Non-crop interference, such as background soil reflectance or surrounding vegetation, may introduce noise that obscures the true radiometric signals from sugarcane canopies (Som-Ard et al., 2021). Such variability makes it challenging to develop generalized models that can accurately capture stress patterns across diverse environments.

4.3 Data processing and integration challenges

The processing of RS data involves extensive pre-processing steps such as atmospheric correction, radiometric calibration, and cloud masking to ensure accuracy, which can be time-consuming and computationally demanding (Som-Ard et al., 2021). Integrating data from multiple sensors or platforms for comprehensive stress assessment requires sophisticated algorithms and standardized analysis-ready data (ARD) formats, which are still evolving. Obtaining reliable ground truth data for model calibration and validation remains another challenge, especially across large or remote agricultural regions.

4.4 Modelling and analytical constraints

ML and deep learning models, though promising, face constraints when applied to heterogeneous agricultural datasets. Unbalanced data distributions, intra-species variability, and

insufficient ground truth samples can reduce model accuracy and generalizability (Kamarudin et al., 2021; Koohi et al., 2023). Effective calibration and validation are essential for improving model reliability across different environmental and management conditions.

Addressing these limitations requires continuous research, technological innovation, and interdisciplinary collaboration among RS scientists, agronomists, data analysts, and policymakers. Ongoing integration of AI and RS approaches holds great potential to overcome current barriers and enhance the precision and scalability of stress detection in sugarcane farming. The present review also emphasizes previous research that combines these emerging technologies to evaluate crop stresses, specifically water, salinity, and nitrogen in sugarcane cultivation systems.

5 Future directions

The future of sustainable agriculture depends on the widespread integration of advanced technologies such as ML, RS, IoT, robotics, PA, and cloud computing. Although these technologies possess immense potential, their adoption particularly in developing regions remains limited. In the context of increasing challenges such as climate change, land degradation, and water scarcity, the deployment of intelligent systems is essential to ensure efficient management of water and nutrient resources during crop production. Real-time monitoring and predictive analytics play a pivotal role in addressing critical stressors such as water deficiency, salinity, and nitrogen imbalance. When applied to RS data, ML techniques can effectively detect spatial variability in water use efficiency, particularly in low-productivity zones, thereby improving irrigation scheduling and enhancing crop management without expanding cultivated land or increasing water consumption. Integration of advanced RS technologies has further revolutionized sugarcane monitoring and management. Hyperspectral imaging enables precise detection of water and nutrient levels, improving the ability to assess crop health and stress conditions (Swami et al., 2025). The use of unmanned aerial vehicles (UAVs) and CubeSats provides high-resolution spatial and temporal data crucial for real-time monitoring of environmental stressors (Swami et al., 2025). Data fusion techniques, which combine information from multiple sensors and platforms, enhance the accuracy of assessing crop conditions and resource availability (Swami et al., 2025). AI-driven predictive modelling further strengthens decision-making in precision agriculture. The ML algorithms enhance the prediction of crop responses to water and nutrient availability, supporting site-specific management strategies (Gupta et al., 2024). Real-time monitoring systems, such as SWARM, dynamically adjust irrigation and nutrient delivery based on live data, optimizing resource use and improving efficiency (Babu et al., 2006).

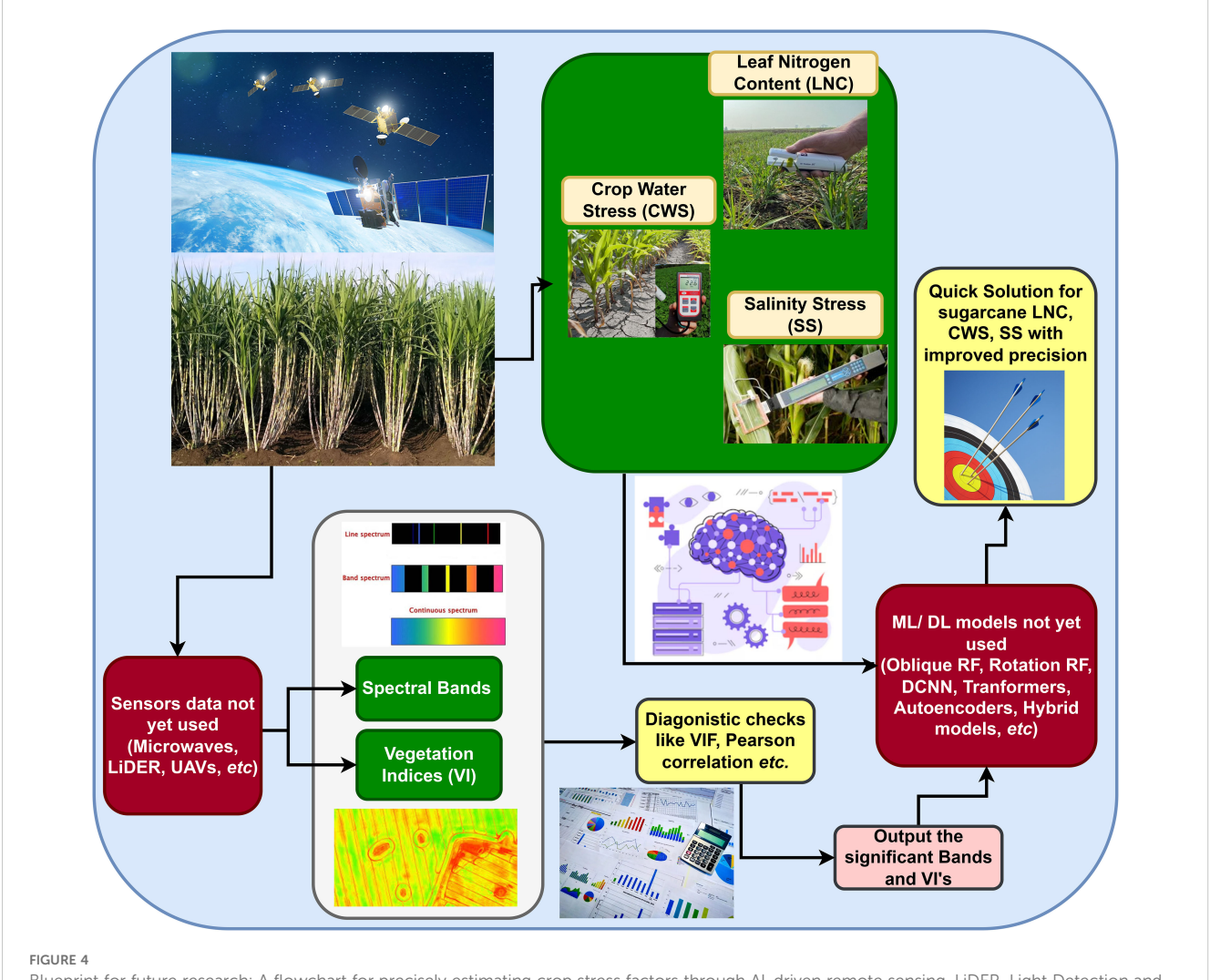
Moreover, coupling RS datasets with ML classification algorithms especially those utilizing full spectral ranges has shown

high accuracy in assessing salinity and nitrogen levels in sugarcane crops. Integrating explainable AI (XAI) approaches is crucial to enhance model transparency and interpretability. XAI provides insights into the decision-making process of ML models, allowing agronomists and farmers to understand which spectral features or environmental factors drive specific predictions. This interpretability builds trust in AI-driven recommendations and promotes informed field management decisions. However, several barriers remain. The high cost of proprietary cognitive farming solutions, coupled with the computational demands of advanced ML algorithms, continues to limit large-scale adoption. To overcome these challenges, the development of open-source, farmer-friendly platforms is essential to democratize access to digital technologies and reduce dependency on expensive commercial software. Furthermore, optimizing ML models to reduce processing time and computational overhead through lightweight algorithms and edge computing will enable integration with RS systems on resource-constrained devices. Future research should also prioritize sensor calibration, data accessibility, and ethical data management, ensuring privacy and equitable use of agricultural data. Establishing clear frameworks for data ownership and protection will foster trust and encourage the broader adoption of AI- and RS-based technologies. Collectively, these innovations will pave the way toward scalable, cost-effective, and sustainable precision management systems for water, salinity, and nutrient optimization in sugarcane cultivation (Figure 4).

6 Concluding remarks

Over the past decade, agricultural systems have increasingly integrated AI and RS technologies to address critical challenges and boost productivity. This review compiles current knowledge on the application of AI and RS in sugarcane cultivation, highlighting their strengths and constraints in managing crop water stress, leaf nitrogen estimation, and salinity stress mapping. Although their adoption in agriculture lags behind other sectors, the continuous evolution of sensors, UAVs, and ML algorithms presents substantial opportunities for innovation in sugarcane farming. Despite these advancements, significant barriers remain - including high initial investment, sensor limitations, complex data processing requirements, limited technical expertise, and farmer apprehension. Nevertheless, AI-driven RS approaches show great promise for improving both yield and quality in sugarcane, while contributing positively to environmental and socioeconomic outcomes.

Conventional soil moisture monitoring methods are often constrained by high sensor costs, installation complexity, and inaccuracies, especially across varied soil types and crop systems. Plant-based assessments, while more reliable and accurate, often lack scalability and are time-intensive. Research consistently shows that remotely sensed indices such as the Photochemical Reflectance Index (PRI) and NDVI are significantly correlated with physiological parameters like leaf water potential (LWP), stomatal



Blueprint for future research: A flowchart for precisely estimating crop stress factors through Al-driven remote sensing. LiDER, Light Detection and Ranging; UAVs, Unmanned Aerial Vehicles; VIF, Variance Inflation Factor; ML, Machine Learning; DL, Deep Learning; RF, Random Forest; DCNN, Deep Convolutional Neural Networks.

conductance, crop coefficient, and stem water potential. However, relying solely on single-parameter metrics for plant water status estimation often falls short in precision. Among water stress indicators, the CWSI, particularly when derived from Earth Observation (EO) data has emerged as a preferred metric for assessing sugarcane water status across local to regional scales. Infrared thermometers continue to serve as effective ground tools for measuring canopy temperature, providing critical validation for RS-based observations. Midday stem water potential also remains a standard reference point for cross-verifying RS-derived estimates. For salinity stress evaluation, studies endorse the use of multispectral (e.g., Landsat ETM+) and hyperspectral (e.g., Hyperion) satellite data, with classification algorithms like minimum distance (MD) consistently delivering reliable results. Nitrogen estimation in sugarcane has similarly benefited from vegetation indices that combine near-infrared, green, and rededge wavelengths. Indices such as SAVI (soil adjusted vegetation index), MSAVI (modified SAVI), NDVI, and OSAVI have been

effectively incorporated into linear, nonlinear, and ML-based models, with ML approaches consistently outperforming traditional methods in accuracy and adaptability.

Among ML techniques, Artificial Neural Networks (ANNs) have shown particular success in analyzing UAV multispectral data and in determining variable contributions to target outcomes. Support Vector Machines (SVM) and Random Forests (RF) also demonstrate high potential in RS-based classification, though their full capabilities in detecting crop stresses specifically water, salinity, and nitrogen are still underexplored. Recent innovations like oblique and rotation-based RF classifiers have exhibited improved performance across varied datasets. The oblique RF approach, effective with discrete factorial features, is promising for evaluating water stress and warrants deeper investigation. Similarly, the rotation RF model, which integrates multiple rotated feature spaces, has surpassed traditional classifiers such as RF, SVM, and k-NN in several studies. Despite this, both rotation RF and deep CNNs remain underutilized in stress

assessment involving RS data sources such as microwave imagery, UAVs, and Light Detection and Ranging (LiDAR). Machine learning's capacity to aggregate and analyze data from diverse sources including ground measurements, sensor networks, meteorological data, and RS platforms like satellites, drones, and airborne systems makes it central to the future of digital agriculture. While ML has been widely applied in tasks such as crop classification, yield prediction, and condition monitoring, more targeted research is needed to fully harness its potential for stress assessments in sugarcane, particularly in water, salinity, and nitrogen dynamics. These areas are vital for informed irrigation planning and sustainable crop management, and thus demand greater attention from the research community. Continued advancements in this field will significantly benefit sugarcane agriculture by enhancing productivity, supporting long-term sustainability, and improving resilience against challenges such as climate variability, resource constraints, and market instability.

Author contributions

V: Conceptualization, Methodology, Data curation, Formal Analysis, Writing – original draft, Writing – review & editing. PP: Conceptualization, Data curation, Supervision, Writing – original draft, Writing – review & editing, Formal Analysis, Methodology. GA: Data curation, Formal Analysis, Methodology, Writing – review & editing, Writing – original draft. A: Data curation, Methodology, Writing – original draft, Writing – review & editing. RA: Conceptualization, Writing – original draft, Writing – review & editing. PM: Conceptualization, Writing – original draft, Writing – original draft, Writing – review & editing. PG: Supervision, Writing – original draft, Writing – review & editing. PG: Supervision, Writing – original draft, Writing – review & editing.

Funding

The author(s) declare that no financial support was received for the research, and/or publication of this article.

References

Abdel-Rahman, E. M., and Ahmed, F. B. (2008). The application of remote sensing techniques to sugarcane (*Saccharum* spp. hybrid) production: A review of the literature. *Int. J. Remote Sens.* 29, 3753–3767. doi: 10.1080/01431160701874603

Abdel-Rahman, E. M., Ahmed, F. B., and Berg, M. (2010). Estimation of sugarcane leaf nitrogen concentration using in *situ* spectroscopy. *Int. J. Appl. Earth Observation Geoinformation* 12, 52–57. doi: 10.1016/j.jag.2009.11.003

Abdel-Rahman, E. M., Ahmed, F. B., and Ismail., R. (2013). Random forest regression and spectral band selection for estimating sugarcane leaf nitrogen concentration using EO-1 Hyperion hyperspectral data. *Int. J. Remote Sens.* 34, 712–728. doi: 10.1080/01431161.2012.713142

Abebe, G., Tadesse, T., and Gessesse., B. (2023). Estimating leaf area index and biomass of sugarcane based on Gaussian process regression using Landsat 8 and Sentinel 1A observations. *Int. J. Image Data Fusion* 14, 58–88. doi: 10.1080/19479832.2022.2055157

Acknowledgments

Research was supported by the Indian Council of Agricultural Research, Department of Agricultural Research and Education, Government of India. The authors thank the editors and reviewers for the critical suggestions that led improvements in the article.

Conflict of interest

Authors GA was employed by Avyagraha Research and Analytics LLP.

The remaining authors declare that the research was conducted in the absence of any commercial or financial relationships that could be construed as a potential conflict of interest.

The handling editor SR declared a past co-authorship with the author(s) GA.

Generative AI statement

The author(s) declare that no Generative AI was used in the creation of this manuscript.

Any alternative text (alt text) provided alongside figures in this article has been generated by Frontiers with the support of artificial intelligence and reasonable efforts have been made to ensure accuracy, including review by the authors wherever possible. If you identify any issues, please contact us.

Publisher's note

All claims expressed in this article are solely those of the authors and do not necessarily represent those of their affiliated organizations, or those of the publisher, the editors and the reviewers. Any product that may be evaluated in this article, or claim that may be made by its manufacturer, is not guaranteed or endorsed by the publisher.

Ahmed, F. B. (2010). Estimation of leaf nitrogen and silicon using hyperspectral remote sensing. *J. Appl. Remote Sens.* 4, 043560. doi: 10.1117/1.3525241

Alavi, M., Albaji, M., Golabi, M., Zareian, M., Ayoubi, S., and Javanmard., R. (2024). Estimation of sugarcane evapotranspiration from remote sensing and limited meteorological variables using machine learning models. *J. Hydrology* 629, 130605. doi: 10.1016/j.jhydrol.2023.130605

Amarasingam, N., Ashan Salgadoe, A. S., Powell, K., Gonzalez, L. F., and Natarajan., S. (2022). A review of UAV platforms, sensors, and applications for monitoring of sugarcane crops. *Remote Sens. Applications: Soc. Environ.* 26, 100712. doi: 10.1016/j.rsase.2022.100712

Amaresh, N., Vinayaka, A., Kumari, S., Avinash, G., Abhishek, G. J., Dhanya, V. G., et al. (2024). "Sugarcane Bagasse: Transforming Waste into Renewable and Bio-Compostable Materials for a Sustainable Future," in *Value Addition and Product Diversification in Sugarcane*. Eds. G. S. Suresha, G. Krishnappa, M. Palanichamy, H. K.

Mahadeva Swamy, H. Kuppusamy and H. Govindakurup (Springer, Singapore). doi: 10.1007/978-981-97-7228-5 12

- Anas, M., Liao, F., Verma, K. K., Sarwar, M. A., Mahmood, A., Chen, Z. L., et al. (2020). Fate of nitrogen in agriculture and environment: Agronomic, eco-physiological and molecular approaches to improve nitrogen use efficiency. *Biol. Res.* 53, 47. doi: 10.1186/s40659-020-00312-4
- Babu, C., Athmaraman, N., Ganesan, A., Soundararajan, S., and Muthukumar, R. (2006). "SWARM: Sensor driven water and agricultural resources management," in 2006 Annual IEEE India Conference. New Delhi, India:IEEE. 1–6. doi: 10.1109/INDCON.2006.302766
- Barros, P. P. D. S., Fiorio, P. R., Demattê, J. A. D. M., Martins, J. A., Montezano, Z. F., and Dias., F. L. F. (2021). Estimation of leaf nitrogen levels in sugarcane using hyperspectral models. *Ciec. Rural* 52. doi: 10.1590/0103-8478cr20200630
- Berni, J. A., Zarco-Tejada, P. J., Suárez, L., Sepulcre-Cantó, F., Morales, D. I., Sobrino, J. M., et al. (2009). Thermal and narrowband multispectral remote sensing for vegetation monitoring from an unmanned aerial vehicle. *IEEE Trans. Geosci. Remote Sens.* 47, 722–738. doi: 10.1109/TGRS.2008.2010457
- Bispo, R. C., Hernandez, F. B. T., Gonçalves, I. Z., Neale, C. M. U., and Teixeira., A. H. C. (2022). Remote sensing-based evapotranspiration modeling for sugarcane in Brazil using a hybrid approach. *Agric. Water Manage.* 271, 107763. doi: 10.1016/j.agwat.2022.107763
- Boschiero, B. N., Mariano, E., Torres-Dorante, L. O., Sattolo, T. M., Otto, R., Garcia, P. L., et al. (2020). Nitrogen fertilizer effects on sugarcane growth, nutritional status, and productivity in tropical acid soils. *Nutrient Cycling* 117, 367–382. doi: 10.1007/s10705-020-10074-w
- Brunini, R. G., and Turco, J. E. (2016). Water stress indices for the sugarcane crop on different irrigated surfaces. *Rev. Bras. Engenharia Agrícola e Ambiental* 20, 925–929. doi: 10.1590/1807-1929/agriambi.v20n10p925-929
- Burt, C. M., and Isbell, B. (2005). Leaching of accumulated soil salinity under drip irrigation. $Trans.\ ASAE\ 48,\ 2115-2121.\ doi:\ 10.13031/2013.20097$
- Chele, K. H., Tinte, M. M., Piater, L. A., Dubery, I. A., and Tugizimana., F. (2021). Soil salinity, a serious environmental issue and plant responses: A metabolomics perspective. *Metabolites* 11, 724. doi: 10.3390/metabol1110724
- Cho, S. B., Soleh, H. M., Choi, J. W., Hwang, W. H., Lee, H., Cho, Y. S., et al. (2024). Recent methods for evaluating crop water stress using ai techniques: A review. *Sensors* 24, 6313. doi: 10.3390/s24196313
- Das, K., Khiripet, N., Chattanrassamee, P., Kijkullert, C., and Veerachit, V. (2020). Crop evapotranspiration estimates for sugarcane based on remote sensing and land surface model in Thailand. 2020 IEEE Int. Geosci. Remote Sens. Symposium (IGARSS), 5175–5178. doi: 10.1109/IGARSS39084-2020
- Dhansu, P., Kumar, R., Kumar, A., Vengavasi, K., Raja, A. K., Vasantha, S., et al. (2022). Differential physiological traits, ion homeostasis, and cane yield of sub-tropical sugarcane varieties in response to long-term salinity stress. *Sustainability* 14, 13246. doi: 10.3390/su142013246
- Djajadi, D., Syaputra, R., and Hidayati., S. N. (2022). "Effect of salt stress on nutrient content in soil and leaves of three sugarcane varieties," in *IOP Conference Series: Earth and Environmental Science*, Vol. 974. 012048. Bogor, Indonesia: IOP Publishing. doi: 10.1088/1755-1315/974/1/012048
- Driemeier, C., Ling, L. Y., Sanches, G. M., Pontes, A. O., Magalhães, P. S. G., and Ferreira., J. E. (2016). A computational environment to support research in sugarcane agriculture. *Comput. Electron. Agric.* 130, 13–19. doi: 10.1016/j.compag.2016.10.002
- FAO (2022). World food and agriculture Statistical yearbook 2022 (FAO) Rome, Italy. doi: 10.4060/cc2211en
- Ferreira, T. H. S., Tsunada, M. S., Bassi, D., Araújo, P., Mattiello, L., Guidelli, G. V., et al. (2017). Sugarcane water stress tolerance mechanisms and its implications on developing biotechnology solutions. *Front. Plant Sci* 8. doi: 10.3389/fpls.2017.01077
- Gai, J., Wang, J., Xie, S., Xiang, L., and Wang, Z.Spectroscopic determination of chlorophyll content in sugarcane leaves for drought stress detection *Precision Agriculture* (2024)25:543–569.doi: 10.1007/s11119-023-10082-0
- Gonçalves, I. Z., Ruhoff, A., Laipelt, L., Bispo, R. C., Hernandez, F. B. T., Neale, C. M. U., et al. (2022). Remote sensing-based evapotranspiration modeling using geeSEBAL for sugarcane irrigation management in Brazil. *Agric. Water Manage.* 274, 107965. doi: 10.1016/j.agwat.2022.107965
- Gopalasundaram, P., Bhaskaran, A., and Rakkiyappan., P. (2012). Integrated nutrient management in sugarcane. *Sugar Tech* 14, 3–20. doi: 10.1007/s12355-011-0097-x
- Grof, C. P. L., and Campbell, J. A. (2001). Sugarcane sucrose metabolism: Scope for molecular manipulation. Funct. Plant Biol. 28, 1. doi: 10.1071/PP00039
- Gupta, D. K., Pagani, A., Zamboni, P., and Singh, A. K. (2024). AI-powered revolution in plant sciences: advancements, applications, and challenges for sustainable agriculture and food security. *Explor. Foods Foodomics* 2, 443–459. doi: 10.37349/eff.2024.00045
- Hamzeh, S., Naseri, A. A., AlaviPanah, S. K., Bartholomeus, H., and Herold, M. (2016). Assessing the accuracy of hyperspectral and multispectral satellite imagery for categorical and quantitative mapping of salinity stress in sugarcane fields. *Int. J. Appl. Earth Observation Geoinformation* 52, 412–421. doi: 10.1016/j.jag.2016.06.024

- Hamzeh, S., Naseri, A. A., AlaviPanah, S. K., Mojaradi, B., Bartholomeus, H. M., Clevers, J. G. P. W., et al. (2013). Estimating salinity stress in sugarcane fields with spaceborne hyperspectral vegetation indices. *Int. J. Appl. Earth Observation Geoinformation* 21, 282–290. doi: 10.1016/j.jag.2012.07.002
- Hamzeh, S., Naseri, A. A., Panah, S. A., Mojaradi, B., Bartholomeus, H. M., and Herold., M. (2012). Mapping salinity stress in sugarcane fields with hyperspectral satellite imagery. *Remote Sens. Agriculture Ecosystems Hydrology XIV* 8531, 528–535. doi: 10.1117/12.981655
- Haq, Y. U., Shahbaz, M., Asif, H. S., Al-Laith, A., and Alsabban, W. H. (2023). Spatial mapping of soil salinity using machine learning and remote sensing in Kot Addu, Pakistan. *Sustainability* 15, 12943. doi: 10.3390/su151712943
- Hellegers, P. J. G. J., Soppe, R., Perry, C. J., and Bastiaanssen., J. (2009). Combining remote sensing and economic analysis to support decisions that affect water productivity. *Irrigation Sci* 27, 243–251. doi: 10.1007/s00271-008-0139-7
- Huang, Y., Chen, Z. X., Tao, Y. U., Huang, X. Z., and Gu., X. F. (2018). Agricultural remote sensing big data: Management and applications. *J. Integr. Agric.* 17, 1915–1931. doi: 10.1016/S2095-3119(17)61859-8
- Idso, S. B., Jackson, R. D., Pinter, P. J., Reginato, R. J., and Hatfield., J. L. (1981). Normalizing the stress-degree-day parameter for environmental variability. *Agric. Meteorology* 24, 45–55. doi: 10.1016/0002-1571(81)90032-7
- Infomerics Valuation and Rating Pvt. Ltd (2024). Sugar Industry Outlook December. Available online at: https://www.infomerics.com/admin/uploads/sugar-industry-dec24.pdf. (Accessed May 25, 2025).
- Inman-Bamber, N. G. (2004). Sugarcane water stress criteria for irrigation and drying off. Field Crops Res. 89, 107–122. doi: 10.1016/j.fcr.2004.01.018
- Kamarudin, M. H., Ismail, Z. H., and Saidi, N. B. (2021). Deep learning sensor fusion in plant water stress assessment: A comprehensive review. *Appl. Sci.* 11, 1403. doi: 10.3390/app11041403
- Kaplan, G., Gašparović, M., Alqasemi, A. S., Aldhaheri, A., Abuelgasim, A., and Ibrahim, M. (2023). Soil salinity prediction using machine learning and sentinel–2 remote sensing data in hyper–arid areas. *Phys. Chem. Earth* 130, 103400. doi: 10.1016/j.pce.2023.103400
- Katsoulas, N., Elvanidi, A., Ferentinos, K. P., Kacira, G., Bartzanas, C., and Kittas., C. K. (2016). Crop reflectance monitoring as a tool for water stress detection in greenhouses: A review. *Biosyst. Eng.* 151, 374–398. doi: 10.1016/j.biosystemseng.2016.10.003
- Koohi, E., Gumiere, S. J., and Bonakdari, H. (2023). "Artificial Intelligence Models for Detecting Spatiotemporal Crop Water Stress in schedule Irrigation: A review," in *EGU General Assembly Conference Abstracts*. Vienna, Austria. EGU–3997. doi: 10.5194/egusphere-egu23-3997
- Kumar, R., Dhansu, P., Kulshreshtha, N., Meena, M. R., Kumaraswamy, M. H., Appunu, C., et al. (2023a). Identification of salinity-tolerant stable sugarcane cultivars using AMMI, GGE and some other stability parameters under multi-environments of salinity stress. *Sustainability* 15, 1119. doi: 10.3390/su15021119
- Kumar, R., Sagar, V., Verma, V. C., Kumari, M., Gujjar, R. S., Goswami, S. K., et al. (2023b). Drought and salinity stresses induced physio-biochemical changes in sugarcane: An overview of tolerance mechanism and mitigating approaches. *Front. Plant Sci* 14. doi: 10.3389/fpls.2023.1225234
- Kumar, R., Vasantha, S., Tayade, A., Anusha, S., Geetha, P., and Hemaprabha., G. (2020). Physiological efficiency of sugarcane clones under water-limited conditions. $Trans.\ ASABE\ 63,\ 133-140.\ doi:\ 10.13031/trans.13550$
- Lebourgeois, V., Chopart, J. L., Bégue, A., Clouvel, R., Courties, J., and Wery., P. (2010). Towards using a thermal infrared index combined with water balance modelling to monitor sugarcane irrigation in a tropical environment. *Agric. Water Manage.* 97, 75–82. doi: 10.1016/j.agwat.2009.08.013
- Li, X., Ba, Y., Zhang, M., Nong, M., Yang, C., and Zhang., S. (2022). Sugarcane nitrogen concentration and irrigation level prediction based on UAV multispectral imagery. *Sensors* 22, 2711. doi: 10.3390/s22072711
- Lofton, J. (2012). Improving nitrogen management in sugarcane production of the Mid-South using remote sensing technology. Louisiana State University and Agricultural and Mechanical College, Baton Rouge, Louisiana, United States.
- Martins, J. A., Fiorio, P. R., Silva, C. A. A. C., Demattê, J. A. M., and Silva Barros., P. P. D. (2024). Application of vegetative indices for leaf nitrogen estimation in sugarcane using hyperspectral data. *Sugar Tech* 26, 160–170. doi: 10.1007/s12355-023-01329-1
- Melo, L. L. D., Melo, V.G.M.L.D., Marques, P. A. A., Frizzone, J. A., Coelho, R. D., Romero, R. A. F., et al. (2022). Deep learning for identification of water deficits in sugarcane based on thermal images. *Agric. Water Manage.* 272, 107820. doi: 10.1016/j.agwat.2022.107820
- Meyer, J. H., Wood, R. A., and Leibbrandt., N. B. (1986). Recent advances in determining the N requirement of sugarcane in the South African sugar industry. *Proc. South Afr. Sugar Technologists' Assoc.* 60, 205–211.
- Milagro Jorrat, M., Araujo, P. Z., and Mele., F. D. (2018). Sugarcane water footprint in the province of Tucumán, Argentina. Comparison between different management practices. *J. Cleaner Production* 188, 521–529. doi: 10.1016/j.jclepro.2018.03.242
- Mohanan, M. V., Pushpanathan, A., Padmanabhan, S., Sasikumar, T., Jayanarayanan, A. N., Selvarajan, D., et al. (2021). Overexpression of *Glyoxalase III* gene in transgenic sugarcane confers enhanced performance under salinity stress. *J. Plant Res.* 134, 1083–1094. doi: 10.1007/s10265-021-01300-9

Mokhele, T. A., and Ahmed, F. B. (2010). Estimation of leaf nitrogen and silicon using hyperspectral remote sensing. *J. Appl. Remote Sens.* 4 (1), 043560. doi: 10.1117/13575741

Palaniswami, C., Gopalasundaram, P., and Bhaskaran., A. (2011). Application of GPS and GIS in sugarcane agriculture. *Sugar Tech* 13, 360–365. doi: 10.1007/s12355-011-0098-9

Palaniswami, C., Viswanathan, R., Bhaskaran, A., Rakkiyappan, P., and Gopalasundaram., P. (2014). Mapping sugarcane yellow leaf disease affected area using remote sensing technique. *J. Sugarcane Res.* 4, 55–61.

Patil, V. C., Jha, S. K., Banerjee, A., and Algat., Y. (2021). "Sugarcane crop water status mapping using Landsat 8 imagery, crop water stress index (CWSI), and metric models," in *International Conference on Sugarcane Research: Sugarcane for Sugar and Beyond (CaneCon-2021)*, Coimbatore, India.

Pawar, M. M., Pawar, M. M., Pawar, P. M., and Deshmukh, B. M. (2024). Advancing sugarcane farm management through NDVI-based color mapping and drone imaging. *Logistic Operation Manage. Res. (LOMR)* 3, 55–68. doi: 10.31098/lomr.v3i2.2824

Pereira, R. M., Casaroli, D., Vellame, L. M., Oliveira, F. A., Rodrigues, R. F., Pires, A. L., et al. (2020). Water deficit detection in sugarcane using canopy temperature from satellite images. *Aust. J. Crop Sci* 14, 400–407. doi: 10.21475/ajcs.20.14.03.p1647

Picoli, M. C. A., MaChado, P. G., Duft, D. G., Gomes, L. M., Fernandes, F. H., Leite, J. E., et al. (2019). Sugarcane drought detection through spectral indices derived modeling by remote-sensing techniques. *Model. Earth Syst. Environ.* 5, 1679–1688. doi: 10.1007/s40808-019-00619-6

Rahman, M. R., Islam, A. H. M. H., and Rahman., M. A. (2004). NDVI derived sugarcane area identification and crop condition assessment. *Plan Plus* 1, 1–12.

Ranjan, R., Chopra, U. K., Sahoo, R. N., Singh, A. K., and Pradahan., S. (2012). Assessment of plant nitrogen stress in wheat (*Triticum aestivum* L.) through hyperspectral indices. *Int. J. Remote Sens.* 33, 6342–6360. doi: 10.1080/01431161.2012.687473

Reyes-Trujillo, A., Daza-Torres, M. C., Galindez-Jamioy, C. A., Rosero-García, E. E., Muñoz-Arboleda, F., and Solarte-Rodriguez., E. (2021). Estimating canopy nitrogen concentration of sugarcane crop using in *situ* spectroscopy. *Heliyon* 7, e06566. doi: 10.1016/j.heliyon.2021.e06566

Simoes, W. L., Oliveira, A. R., Tardin, F. D., Brito, J. S., de Souza, A. P., and Ribeiro., R. V. (2023). Saline stress affects the growth of *Saccharum* complex genotypes. *J. Agron. Crop Sci* 209, 613–618. doi: 10.1111/jac.12647

Singels, A., Jarmain, C., Bastidas-Obando, E., and Annandale., J. (2018). Monitoring water use efficiency of irrigated sugarcane production in Mpumalanga, South Africa, using SEBAL. *Water SA* 44, 636–646. doi: 10.4314/wsa.v44i4.12

Singels, A., Van Den Berg, M., Smit, M. A., Jones, S., Bezuidenhout, P., and Van Antwerpen., M. (2010). Modelling water uptake, growth, and sucrose accumulation of sugarcane subjected to water stress. *Field Crops Res.* 117, 59–69. doi: 10.1016/j.fcr.2010.02.003

Soltanikazemi, M., Minaei, S., Shafizadeh-Moghadam, H., and Mahdavian., A. (2022). Field-scale estimation of sugarcane leaf nitrogen content using vegetation indices and spectral bands of Sentinel-2: Application of random forest and support vector regression. *Comput. Electron. Agric.* 200, 107130. doi: 10.1016/j.compag.2022.107130

Som-Ard, J., Atzberger, C., Izquierdo-Verdiguier, E., Vuolo, F., and Immitzer, M. (2021). Remote sensing applications in sugarcane cultivation: A review. *Remote Sens.* 13, 4040. doi: 10.3390/rs13204040

Sundara, B., Natarajan, V., and Hari., K. (2002). Influence of phosphorus solubilizing bacteria on the changes in soil available phosphorus and sugarcane and sugar yields. *Field Crops Res.* 77, 43–49. doi: 10.1016/S0378-4290(02)00048-5

Suresha, G. S., Hari, K., Murali, P., Rajamani, L., Kalaiselvi, K., Gopalareddy, K., et al. (2024). "Sugarcane Fibre as Dietary Supplement, Health Benefits and Applications in Functional Foods," in *Value Addition and Product Diversification in Sugarcane*. Eds. G. S. Suresha, G. Krishnappa, M. Palanichamy, H. K. Mahadeva Swamy, H. Kuppusamy and H. Govindakurup (Springer, Singapore). doi: 10.1007/978-981-97-7228-5_17

Swami, P., Anusha, M., David, K. M., Saivamsireddy, G., Upadhyay, L., and Panigrahi, C. K. (2025). Innovations in remote sensing techniques for monitoring

agricultural crops and environmental stress conditions: A review. J. Sci. Res. Rep. 31, 178–194. doi: 10.9734/isrr/2025/v31i63120

Tayade, A., Vasantha, S., Anusha, S., Kumar, R., and Hemaprabha, G. (2020). Irrigation water use efficiency and water productivity of commercial sugarcane hybrids under water-limited conditions. *Trans. ASABE* 63, 125–132. doi: 10.13031/trans.13548

Teixeira, A. D. C., Leivas, J. F., Ronquim, C. C., Ferreira, L. G., Moreira, E. F., and dos Santos., J. P. (2016). Sugarcane water productivity assessments in the São Paulo State, Brazil. *Int. J. Remote Sens. Appl.* 6, 84–95.

Triadi, R., Herdiyeni, Y., and Tarigan., S. D. (2020). "Estimating crop water stress of sugarcane in Indonesia using Landsat 8," in 2020 International Conference on Computer Science and Its Application in Agriculture (ICOSICA). 1–4. Bogor, Indonesia. doi: 10.1109/ICOSICA49951.2020.9243255

Vasantha, S., and Gomathi, R. (2012). Growth and development of sugarcane under salinity. *J. Sugarcane Res.* 2, 1–10.

Veysi, S., Naseri, A. A., Hamzeh, S., and Eftekhari., A. (2017). A satellite-based crop water stress index for irrigation scheduling in sugarcane fields. *Agric. Water Manage*. 189, 70–86. doi: 10.1016/j.agwat.2017.04.016

Veysi, S., Naseri, A. A., Hamzeh, S., Mohammadzadeh, A., Karami, M., and Mojaradi., B. (2020). Relationship between field measurement of soil moisture in the effective depth of sugarcane root zone and extracted indices from spectral reflectance of optical/thermal bands of multispectral satellite images. *J. Indian Soc. Remote Sens.* 48, 1035–1044. doi: 10.1007/s12524-020-01135-2

Vinayaka,, and Prasad, P. R. C. (2024). AI-enhanced remote sensing applications in Indian sugarcane research: A comprehensive review. *Sugar Tech* 26, 609–628. doi: 10.1007/s12355-024-01409-w

Virnodkar, S. S., Pachghare, V. K., Patil, V. C., and Jha., S. K. (2020). Remote sensing and machine learning for crop water stress determination in various crops: A critical review. *Precis. Agric.* 21, 1121–1155. doi: 10.1007/s11119-020-09711-9

Virnodkar, S. S., Pachghare, V. K., Patil, V. C., and Jha., S. K. (2021). Denseresunet: An architecture to assess water-stressed sugarcane crops from Sentinel-2 satellite imagery. *Trait du Signal* 38, 1131–1139. doi: 10.18280/ts.380424

Vu, N.-T., Bui, T.-K., Vu, T.-T.-H., Nguyen, T.-H., Le, T.-T.-C., Tran, A.-T., et al. (2023). Biochar improved sugarcane growth and physiology under salinity stress. *Appl. Sci.* 13, 7708. doi: 10.3390/app13137708

Waqas, M. M., Awan, U. K., Cheema, M. J. M., Ahmad, I., Ahmad, M., Ali, S., et al. (2019). Estimation of canal water deficit using satellite remote sensing and GIS: A case study in Lower Chenab Canal System. *J. Indian Soc. Remote Sens.* 47, 1153–1162. doi: 10.1007/s12524-019-00977-9

Watanabe, K., Agarie, H., Aparatana, K., Mitsuoka, M., Taira, E., Ueno, M., et al. (2022). Fundamental study on water stress detection in sugarcane using thermal image combined with photosynthesis measurement under a greenhouse condition. *Sugar Tech* 24, 1382–1390. doi: 10.1007/s12355-021-01087-y

Waters, E. K., Chen, C. C. M., and Azghadi, M. R. (2025). Sugarcane health monitoring with satellite spectroscopy and machine learning: A review. *Comput. Electron. Agric.* 229, 109686. doi: 10.1016/j.compag.2024.109686

Wiedenfeld, R. P. (1995). Effects of irrigation and N fertilizer application on sugarcane yield and quality. *Field Crops Res.* 43, 101–108. doi: 10.1016/0378-4290 (95)00043-P

Wood, A. W., Muchow, R. C., and Robertson., M. J. (1996). Growth of sugarcane under high input conditions in tropical Australia. III. Accumulation, partitioning, and use of nitrogen. *Field Crops Res.* 48, 223–233. doi: 10.1016/S0378-4290(96)00043-3

Yang, Y., Gao, S., Jiang, Y., Lin, Z., Luo, J., Li, M., et al. (2019). The physiological and agronomic responses to nitrogen dosage in different sugarcane varieties. *Front. Plant Sci* 10. doi: 10.3389/fpls.2019.00406

Yang, H., Shukla, M. K., Mao, X., Kang, S., and Du., T. (2019). Interactive regimes of reduced irrigation and salt stress depressed tomato water use efficiency at leaf and plant scales by affecting leaf physiology and stem sap flow. *Front. Plant Sci* 10. doi: 10.3389/fpls.2019.00160

Yueanket, A., Phunklang, S., Kornsing, S., Kupimai, M., Innok, A., Pumpoung, T., et al. (2024). "AIoT-based water management solutions for sustainable sugarcane farming," in 2024 International Conference on Power, Energy and Innovations (ICPEI). 19–23. Nakhon Ratchasima, Thailand. doi: 10.1109/ICPEI61831.2024.10748644